Dynamical spin susceptibility of silicene

Surajit Sarkar and Suhas Gangadharaiah
Department of Physics, Indian Institute of Science Education and Research, Bhopal 462066, India

(Received 27 September 2018; revised manuscript received 11 February 2019; published 11 April 2019)

We present a detailed study of the imaginary and real parts of the spin susceptibility of silicene which can be generalized to other buckled honeycomb structures. We find that while the off-diagonal components are nonzero in individual valleys, they add up to zero upon including contributions from both the valleys. We investigate the interplay of the spin-orbit interaction and an external electric field applied perpendicular to the substrate and find that although the xx and yy components of the susceptibility are identical, they differ from the zz component. The external electric field plays an important role in modifying the allowed intersubband regions. In the dynamic limit, the real part of the susceptibility exhibits log divergence, the position of which can be tuned by the electric field and therefore has implications for spin-collective excitations. The effect of the electric field on the static part of the susceptibility and its consequence for the long distance decay of the spin susceptibility have been explored.

DOI: 10.1103/PhysRevB.99.155122

I. INTRODUCTION

Spin-orbit (SO) interaction is one of the key ingredients in a spintronics device required for controlling and manipulating the spin degrees of freedom of an electron via the electric field [1,2]. In this regard, enormous progress has already been made in the study of semiconductor based spintronics devices [1,3]. Recently the possibility of graphene and other 2D materials, in particular silicene and germanene [4], topological insulators [5,6], Weyl semimetals [7–9], along with monolayer transition metal dichalcogenides such as MoS_2 [10] with intrinsic and extrinsic SO coupling, have garnered wide attention from the fundamental physics point of view as well as for their potential for spintronics applications.

The low energy effective theory of many of these new materials is governed by the Dirac physics. In graphene, due to the relatively small mass of carbon atoms the SO coupling is very weak therefore the physics is effectively described by the massless Dirac theory. The conduction and valance bands meet at the two inequivalent Dirac points, called the K and K′ points, which is where the Fermi energy also lies. On the other hand, due to the higher mass of silicon atoms SO coupling in silicene is appreciable ($\sim$3.9 meV) [11–13]. Unlike graphene which is completely planar, silicene has a buckled honeycomb sublattice structure resulting in the explicit breaking of inversion symmetry [14]. An electric field applied perpendicular to the silicene surface leads to a staggered potential which in combination with the SO term determines the gap in the energy spectrum. Consequently, electric field can be used as a control parameter to drive silicene from a trivial band insulator phase to symmetry protected topological phase (e.g., spin Hall insulator [15,16]). At the critical point the band gap closes [17,18] and silicene enters into a valley-spin polarized metallic state [19–21]. These features in the energy spectrum provide the possibility for detecting quantum, anomalous, and valley hall effects in silicene [19,22,23].

Useful insights into the electronic properties of materials are obtained by studying their charge response function or the charge polarization operator. It yields information regarding the single particle and collective excitations which are crucial for understanding the static and dynamical properties of many body systems [24,25]. While the modifications to the response function due to the SO coupling in 2DEG with parabolic dispersion have been investigated in great detail [26,27], it is only recently that similar studies on the charge response function of materials with Dirac-like dispersion have been made [5–9,28–35]. There have also been studies on the spin response of the SO coupled 2D electron system and of the helical surface states of a 3D topological insulator [5,36–39]. By considering the dynamical spin susceptibility of the SO coupled 2D electron system the existence of spin-collective excitations was established [39], moreover, the surface states of a 3D topological insulator, described by the Dirac spectrum, have been predicted to host hybridized spin-charge coupled plasmons [5]. On the other hand, the modifications to the static spin susceptibility due to the SO terms yield additional interaction terms like Dzyaloshinskii-Moriya and Ising terms besides the usual isotropic Rudermann-Kittel-Kasuya-Yosida (RKKY) interaction term [40–42].

Experimental measurements of spin susceptibility are routinely performed via nuclear resonance and electron spin resonance techniques, which yield Knight-shift and g-factor values, respectively [43–45]. In addition, studies of Shubnikov-de Haas oscillations in high-mobility Si-MOS samples [46] and AlAs quantum wells [47,48] have yielded important information related to correlation effects on the spin susceptibility in these systems. Moreover a scattering cross section obtained in a neutron scattering experiment reveals the structure factor which is directly proportional to the imaginary part of the susceptibility [49]. Recently, Raman spectroscopy techniques were used to reveal the collective spin excitations of the chiral surface states of the three-dimensional topological insulator Bi_2Se_3 [50].

Recent theoretical studies of the charge polarization function of silicene have predicted the existence of charge

collective excitation with a $\sqrt{q}$ dispersion at small q [20,51,52]. However, the study of spin collective modes in silicene and other buckled honeycomb lattice is an ongoing and challenging work. As a first step towards the better understanding of the role of spin-orbit interaction in silicene we study in detail the spin susceptibility in the noninteracting limit. We find that the interplay of inversion symmetric spin-orbit term and the inversion breaking electric field term is responsible for different spin-susceptibility value for the diagonal zz component as compared to the xx and yy components. We discuss in detail the allowed single-particle transitions and the regions in the (q, ω) plane where the imaginary part of the susceptibility is nonzero. The role of electric field in extending the allowed regions for particle-hole excitations is examined. We calculate the real part of susceptibility, with particular emphasis on the dynamic and static limits. We show that the real part of spin susceptibility exhibits log divergence in the dynamic limit (in the xx and yy channels) and discuss its significance with regard to the spin-collective modes. The static part of the spin susceptibility exhibits Kohn anomaly; interestingly the nature of this anomaly and the momentums at which this happens can be controlled by electric field. The consequence of it for the long distance decay behavior of the spin susceptibility has been studied.

Our paper is organized as follows: In Sec. II we provide a general description of our model along with the low energy effective Hamiltonian of silicene. In Sec. III we define the spin-susceptibility operator. In Sec. IV we obtain the contributions to the imaginary part of the spin susceptibility arising from different transition scenarios. In Sec. V the real part of the spin susceptibility in the dynamical and static limits have been calculated. A summary of the results is provided in Sec. VI.

II. MODEL

The tight binding Hamiltonian of 2D silicene is given by

$$H = -t \sum_{\langle i,j\rangle\alpha} \hat{c}^{\dagger}_{i\alpha}\, \hat{c}_{j\alpha} + i\frac{\lambda_{SO}}{3\sqrt{3}} \sum_{\langle\langle i,j\rangle\rangle\alpha\beta} \nu_{ij} \hat{c}^{\dagger}_{i\alpha} \hat{\sigma}^{\alpha\beta}_{z}\, \hat{c}_{j\beta} + l \sum_{i\alpha} \zeta_i E^{i}_{z} \hat{c}^{\dagger}_{i\alpha}\, \hat{c}_{i\alpha} \; - \mu \sum_{i\alpha} \hat{c}^{\dagger}_{i\alpha}\, \hat{c}_{i\alpha}\,, \tag{1}$$

where the first term represents the nearest-neighbor hopping on the honeycomb lattice, and the second term represents the effective SO term which couples next-nearest-neighbor sites. The coupling parameter is denoted by λ_{SO}, $\hat{\sigma}_z$ is the Pauli spin matrix, and $\nu_{ij} = \hat{z} \cdot (\vec{d}_i \times \vec{d}_j)/|\vec{d}_i \times \vec{d}_j|$ with $\vec{d}_i$ and $\vec{d}_j$ being the bonds between the two next-nearest-neighbor sites. The third term represents the staggered sublattice potential, where $\zeta_i = \pm 1$ for the A(B) sites and $2l$ is the separation between the A and B sublattices in the z direction, E_z is an applied electric field perpendicular to the plane and μ is the chemical potential. For silicene $t = 1.6$ eV, $\lambda_{SO} = 3.9$ meV, and $l = 0.23$ Å [14,19,53]. The Hamiltonian receives an additional contribution due to the Rashba SO term, however, the magnitude of this term ($\lambda_R = 0.7$ meV) is almost an order of magnitude less than λ_{SO}. Moreover, near the Dirac points the Rashba term is given by the linear $\sim\lambda_R k$ term which can be neglected when describing the low-energy physics [19,53].

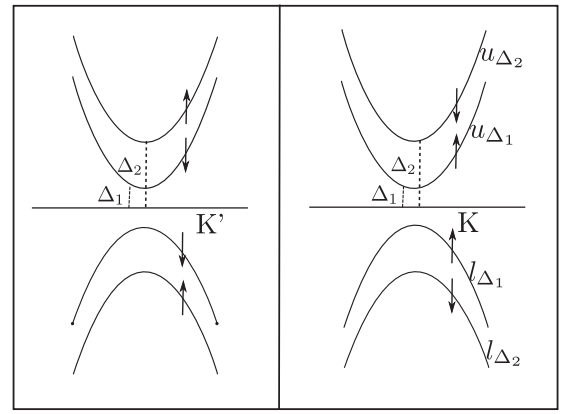

FIG. 1. Energy spectrum near the K and K′ points. The arrows indicate the orientation of the spin in the respective band.

We note that germanene which has a buckled structure is also described by the Hamiltonian given in Eq. (1), with $t = 1.3$ eV, $\lambda_{SO} = 43$ meV, and $l = 0.33$ Å [4,14,19,53]; here also the Rashba term can be neglected when describing the low energy physics.

The low-energy effective Hamiltonian about the two inequivalent Dirac points K_η (where $\eta = \pm 1$) in the basis $(\psi_{A\uparrow}, \psi_{B\uparrow}, \psi_{A\downarrow}, \psi_{B\downarrow})$ acquires the form

$$H_\eta = \hbar v_F (k_x(\hat{I} \otimes \hat{\tau}_x) - \eta k_y(\hat{I} \otimes \hat{\tau}_y)) - \eta\lambda_{SO}\hat{\sigma}_z \otimes \hat{\tau}_z + lE_Z(\hat{I} \otimes \hat{\tau}_z), \tag{2}$$

where the Pauli matrix $\hat{\tau}$ acts on the sublattice basis and η is the valley index. Henceforth, we will set $v_F = 1$ and $\hbar = 1$. The spin-orbit term generates the Kane-Mele mass term $\hat{\sigma}_z \otimes \hat{\tau}_z$ which is time-reversal symmetric and does not break the inversion symmetry; on the other hand the electric field term $\hat{I} \otimes \hat{\tau}_z$ breaks inversion symmetry. Interestingly, in the presence of only one of the terms, either the spin-orbit or the electric field term, the upper and lower bands in each of the valleys are doubly degenerate. However, in the presence of both the terms the band degeneracy is lifted and the spectrum is given by $\epsilon_{k_{\eta\beta}} = \alpha\sqrt{k^2 + \Delta^2_{\eta,\beta}}$, where $\alpha = \pm 1$ and the inequivalent gaps for spins $\beta = \pm 1$ are given by $\Delta_{\eta,\beta} = |lE_z - \eta\beta\lambda_{SO}|$. In Fig. 1 we plot the energy spectrum near the K, K′ points, where the energy gaps are labeled as $\Delta_{1/2} = |lE_z \mp \lambda_{SO}|$. Since spin is a good quantum number we identify the bands having Δ_1 gap in the K (K′) valley with up-spin (down-spin) and similarly the Δ_2 gap in the K (K′) valley with down-spin (up-spin). The strength of the gap can be tuned by external electric field, in particular, for the critical field $E^c_z = \lambda_{SO}/l$ the Hamiltonian exhibits gapless modes. For convenience, the bands are labeled as follows: upper and lower bands with band gap $\Delta_{1/2}$ as $u_{\Delta_{1/2}}$ and $l_{\Delta_{1/2}}$, respectively.

III. GENERALIZED SUSCEPTIBILITY

The noninteracting generalized susceptibility in the Matsubara formalism is given by [39]

$$\chi_{ij}(q, \omega_n) = -\int_P \mathrm{Tr}[\hat{\sigma}_i\, \hat{G}_P\, \hat{\sigma}_j\, \hat{G}_{P+Q}], \tag{3}$$

where Tr denotes trace over spin and sublattice degrees of freedom, $i, j = 0, x, y, z$, $P = (\vec{p}, \Omega_n)$, and $Q = (\vec{q}, \omega_n)$. Note that the polarization function/operator is related to the susceptibility via the relation, $\Pi_{ij}(q, \omega_n) = -\chi_{ij}(q, \omega_n)$. In the rest of the text we will be using the two terms interchangeably.

The corresponding zero temperature Matsubara Green's function used in the above equation has the following form

$$\hat{G}_p = \frac{1}{4} \sum_{\beta,\alpha=\pm1} \frac{\left[(\hat{I} + \beta\hat{\sigma}_z) \otimes \left(\hat{I} - \alpha\left(\vec{p}_\beta \cdot \vec{\tau}\right)/E_{p_\beta}\right)\right]}{\left(i\Omega_n + \alpha E_{p_\beta}\right)}, \quad (4)$$

where $\alpha = \pm 1$ represents lower and upper bands, respectively, $\vec{p}_{\eta\beta} = p_x\hat{e}_1 + \eta p_y\hat{e}_2 + \Delta_{\eta,\beta}\hat{e}_3$, and $E_{p_{\eta\beta}} = |\epsilon_{p_{\eta\beta}}|$. Following the usual procedure for frequency summation, followed by the analytical continuation $i\omega \to \omega + i0^+$, the polarization function of the η valley acquires the form,

$$\Pi^{\eta}_{ij}(q, \omega) = -\frac{1}{4} \int \frac{d^2p}{(2\pi)^2} \sum_{\substack{\alpha,\,\alpha'=\pm1 \\ \beta,\,\beta'=\pm1}} \left[F^{\beta,\beta'}_{i,j} \cdot S^{\alpha,\alpha',\beta,\beta'}_{p,p+q}\right] \times \frac{n_F\left(-\alpha E_{p_{\eta\beta}}\right) - n_F\left(-\alpha' E_{(p+q)_{\eta\beta'}}\right)}{\left(\alpha E_{p_{\eta\beta}} - \alpha' E_{(p+q)_{\eta\beta'}} - \omega - i0^+\right)}, \quad (5)$$

where the prefactors are $F^{\beta,\beta'}_{i,j} = [\delta_{ij}(1 - \beta\beta') + i\epsilon_{izj}(\beta - \beta') + 2\beta\beta'\delta_{iz}\delta_{jz}]$ with $(i, j) \in (x, y, z)$, $F^{\beta,\beta'}_{0,j} = F^{\beta,\beta'}_{j,0} = (\beta + \beta')\delta_{zj}$, and $F^{\beta,\beta'}_{0,0} = (1 + \beta\beta')$. The form factor is given by

$$S^{\alpha,\alpha',\beta,\beta'}_{p,p+q} = \left[1 + \alpha\alpha' \frac{\vec{p}_{\eta\beta} \cdot (\vec{p} + \vec{q})_{\eta\beta'}}{E_{p_{\eta\beta}} E_{(p+q)_{\eta\beta'}}}\right]. \quad (6)$$

The full polarization function is given by the sum, $\Pi_{ij}(q, \omega) = \Pi^{+}_{ij}(q, \omega) + \Pi^{-}_{ij}(q, \omega)$. We note that the off-diagonal components, $\Pi^{\eta}_{0z}(q, \omega)$ and $\Pi^{\eta}_{xy}(q, \omega)$, are nonzero in individual valleys, however, they add up to zero upon including contributions from both the valleys. This could be understood in the following way: for $\Pi^{\pm}_{xy}$ the allowed transitions are between Δ_1 to Δ_2, and vice versa. Focusing only on the $\Delta_1 \to \Delta_2$ (or $\Delta_2 \to \Delta_1$) transition, all terms in the expression of $\Pi^{\pm}_{xy}$ remain the same except the $i(\beta' - \beta)$ term which has opposite signs for the two valleys, thus the cancellation. Similar arguments hold for the vanishing of $\Pi^{\pm}_{0z}$ term after including contributions from both the valleys. On the other hand, the diagonal components obtain equal contributions from both the valleys.

In the following two sections we present in detail the imaginary and real part of spin susceptibility and its characteristic behavior with respect to the external electric field.

IV. IMAGINARY PART OF SUSCEPTIBILITY

We will next focus our attention on the imaginary part of the generalized susceptibility, in particular those arising from χ_{xx} and χ_{yy} (both of which yield the identical result). The charge susceptibility χ_{00} result has already been discussed in the literature [20,31,32,52,54] and the χ_{zz} result follows trivially from those of the χ_{00}. The imaginary part of the spin susceptibility is nonzero in regions where the particle-hole excitations are allowed. For χ_{xx} and χ_{yy}, the contribution to their imaginary parts are obtained by particle transition between bands with opposite spin sectors ($\Delta_{2/1} \to \Delta_{1/2}$) following the relation $\beta\beta' = -1$, and these could be due to both the transitions between upper bands or from lower to upper band.

On the other hand, χ_{zz} obtains contribution from spin-conserving transitions, i.e., $\Delta_{1/2} \to \Delta_{1/2}$. As discussed earlier, in the presence of both the Kane-Mele mass term and electric field, the band degeneracy is lifted resulting in two inequivalent gaps $\Delta_1 \neq \Delta_2$, therefore χ_{zz} obtains different contributions from the other two diagonal terms.

The calculations presented here are for the K valley; the contribution from the K′ valley is identical. We discuss in detail the allowed single-particle transitions for all three possible cases and the regions in the (q, ω) plane where the imaginary part of the susceptibility is nonzero.

A. Imaginary part of $\chi_{xx/yy}$

In the next two subsections, we will separately obtain contributions arising from $\Delta_{2/1} \to \Delta_{1/2}$ transitions, which when combined together give full contribution to χ_{xx} and χ_{yy} from the K valley.

1. ($\Delta_2 \to \Delta_1$) transition

The transition from u_{Δ_2} to u_{Δ_1} is allowed for particles with energy ϵ in the range: $\max[\mu - \omega, \Delta_2] < \epsilon < \mu$. The angular integration of Eq. (5) (with $\alpha = \alpha' = -1$) yields

$$\mathrm{Im}\Pi^{uu}_{21}(q, \omega) = -\mathrm{Re}\left[\frac{1}{\sqrt{q^2 - \omega^2}} \int_{L_x}^{U_x} \frac{dx}{8\pi} \frac{(x - \omega_1)^2 - \gamma_0}{\sqrt{x^2 - \xi^2_{21}}}\right],$$

where $\gamma_0 = q^2 + \Delta_d^2$, $\omega_1 = \omega(\gamma_{21} - 1)$, $\xi_{21} = \sqrt{q^2\gamma^2_{21} + 4q^2\Delta_2^2/(q^2 - \omega^2)}$, $\gamma_{21} = 1 - \Delta_s\Delta_d/(q^2 - \omega^2)$, along with the redefined parameter $\Delta_s = \Delta_2 + \Delta_1$ and $\Delta_d = \Delta_2 - \Delta_1$. Performing the integration by taking the limits of integration to be $U_x = 2\mu + \omega\gamma_{21}$ and $L_x = 2\max[\mu - \omega, \Delta_2] + \omega\gamma_{21}$, we obtain

$$\mathrm{Im}\Pi^{uu}_{21}(q, \omega) = -\frac{1}{4\pi} \frac{1}{\sqrt{q^2 - \omega^2}} \times \begin{Bmatrix} G^{uu}_{21}(2\mu + \omega\gamma_{21}) - G^{uu}_{21}(2\max[\mu - \omega, \Delta_2] + \omega\gamma_{21}) & :1\mathrm{A} \\ G^{uu}_{21}(2\mu + \omega\gamma_{21}) - G^{uu}_{21}(\xi_{21}) & :2\mathrm{A} \end{Bmatrix},$$

where

$$G^{uu}_{21}(x) = \tfrac{1}{4}\left\{\left[-2q^2 - 2\Delta_d^2 + \xi^2_{21} + 2(\omega\gamma_{21} - \omega)^2\right] \log\left(\sqrt{x^2 - \xi^2_{21}} + x\right) + \left[x - 4(\omega\gamma_{21} - \omega)\right]\sqrt{x^2 - \xi^2_{21}}\right\}. \quad (7)$$

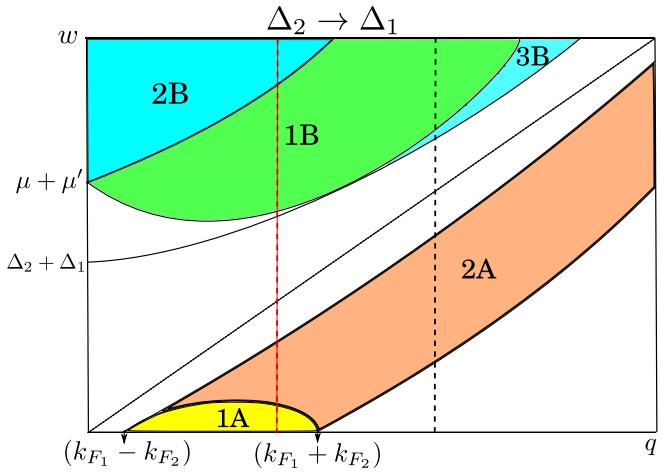

FIG. 2. Shaded regions in the figure indicate nonzero contributions to the imaginary part of the polarization function due to the $\Delta_2 \to \Delta_1$ transition. 1A and 2A regions denote contributions from the transitions u_{Δ_2} to u_{Δ_1}, whereas 1B, 2B, and 3B denote contributions from l_{Δ_2} to u_{Δ_1}. Here $\mu' = \sqrt{k_{F_1}^2 + \Delta_2^2}$, $k_{F_1} = \sqrt{\mu^2 - \Delta_1^2}$, and $k_{F_2} = \sqrt{\mu^2 - \Delta_2^2}$.

The regions in the (q, ω) plane where $\mathrm{Im}\Pi_{21}^{uu}(q, \omega)$ is nonzero are [see Fig. 2]:

$$1A : \omega < \mu - \mathcal{F}\big(k_{F_1}, \Delta_2\big)$$

$$2A : \pm\mu \mp \mathcal{F}\big(k_{F_{1(2)}}, \Delta_{2(1)}\big) < \omega < -\mu + \mathcal{F}\big(-k_{F_2}, \Delta_1\big),$$

where $\mathcal{F}(x, y) = \sqrt{(q - x)^2 + y^2}$. The allowed regions for particle-hole (p-h) excitation in the (q, ω) plane can be obtained via kinematic consideration (see the $\omega < q$ region in Fig. 2). For example, in the scenario being discussed, the minimum momentum required for p-h generation is $k_{F_1} - k_{F_2}$; this involves the collinear transition of a particle from the Fermi level of u_{Δ_2} to the Fermi level of u_{Δ_1} without a change in energy. Indeed, the particle's energy need not change for the transition from the Fermi level of one band to the Fermi level of the other band, thus the maximum momentum change for such a process is $k_{F_2} + k_{F_1}$. For a given momentum $q > k_{F_1} - k_{F_2}$, the energy upper bound for a transition from u_{Δ_2} to u_{Δ_1} is $\omega_{\max} = \sqrt{(k_{F_2} + q)^2 + \Delta_1^2} - \mu$. The process involves a particle getting excited from the Fermi level of u_{Δ_2} to an unoccupied level of u_{Δ_1} with the final direction being the same as the initial one. On the other hand the lower boundary (for $q > k_{F_1} + k_{F_2}$) is set by transition involving backscattering of a particle from the Fermi level of u_{Δ_2} to u_{Δ_1} (with momentum change $q - k_{F_2}$) which requires $\omega_{\min} = \sqrt{(k_{F_2} - q)^2 + \Delta_1^2} - \mu$.

A lower, l_{Δ_2}, to upper band u_{Δ_1} transition requires the particle to have energy ϵ in the range: $\mu - \omega < \epsilon < -\Delta_2$. Performing the angular integration of Eq. (5) yields

$$\mathrm{Im}\Pi_{21}^{lu}(q, w) = -\mathrm{Re}\left[\frac{1}{\sqrt{\omega^2 - q^2}} \int_{L_x}^{U_x} \frac{dx}{8\pi} \frac{\gamma_0 - (x + w_1)^2}{\sqrt{\xi_{21}^2 - x^2}}\right],$$

where the limits of integration are $U_x = 2(\omega - \mu) - \omega\gamma_{21}$ and $L_x = 2\Delta_2 - \omega\gamma_{21}$. Integrating the above equation we obtain the following result:

$$\mathrm{Im}\Pi_{21}^{lu}(q, \omega) = -\frac{1}{4\pi} \frac{1}{\sqrt{\omega^2 - q^2}} \times \begin{Bmatrix} G_{21}^{lu}(2(\omega - \mu) - \omega\gamma_{21}) - G_{21}^{lu}(-\xi_{21}) & :1\mathrm{B} \\ G_{21}^{lu}(\xi_{21}) - G_{21}^{lu}(-\xi_{21}) & :2\mathrm{B} \\ G_{21}^{lu}(\xi_{21}) - G_{21}^{lu}(-\xi_{21}) & :3\mathrm{B} \end{Bmatrix},$$

where

$$G_{21}^{lu}(x) = \frac{1}{4}\left\{\left[2q^2 + 2\Delta_d^2 - \xi_{21}^2 - 2(\omega\gamma_{21} - \omega)^2\right] \tan^{-1}\left(\frac{x}{\sqrt{\xi_{21}^2 - x^2}}\right) + [x - 4(\omega\gamma_{21} - \omega)]\sqrt{\xi_{21}^2 - x^2}\right\}. \tag{8}$$

The nonzero regions in the (q, ω) plane are described by the following equations

$$1B : \mu + \mathcal{F}\big(k_{F_1}, \Delta_2\big) < \omega < \mu + \mathcal{F}\big(-k_{F_1}, \Delta_2\big)$$

$$2B : \omega > \mu + \mathcal{F}\big(-k_{F_1}, \Delta_2\big)$$

$$3B : \sqrt{q^2 + \Delta_s^2} < \omega < \mu + \mathcal{F}\big(k_{F_1}, \Delta_2\big).$$

Unlike the transitions involving only the upper bands, $q = 0$ particle-hole transitions are now allowed for all frequencies $\omega > \mu + \sqrt{k_{F_1}^2 + \Delta_2^2}$ (see the $\omega > q$ region in Fig. 2). As q is increased, the threshold frequency given by $\omega = \mu + \sqrt{(k_{F_1} - q)^2 + \Delta_2^2}$ exhibits a downturn; these are realized by processes involving a particle with momentum $p < k_{F_1}$ moving to the upper Fermi level while maintaining its initial direction. For the above process, the minimum allowed frequency $\omega = \mu + \Delta_2$ is reached for $q = k_{F_1}$, where the transitioning particle originally had momentum $p = 0$. Increasing q further, the threshold frequency exhibits an upturn. The process now involves a particle from l_{Δ_2} moving to the upper Fermi level by changing its initial direction. A further increase in q changes the threshold frequency to $\omega = \sqrt{q^2 + \Delta_s^2}$ and is obtained by minimizing $\sqrt{(p - q)^2 + \Delta_2^2} + \sqrt{p^2 + \Delta_1^2}$ with respect to p.

Combining $\mathrm{Im}\Pi_{21}^{uu}$ and $\mathrm{Im}\Pi_{21}^{lu}$ yields the contribution to the imaginary part of the polarization operator from the $2 \to 1$ processes represented as $\mathrm{Im}\Pi_{21}$. In Fig. 3 we have plotted $\mathrm{Im}\Pi_{21}$ as a function of ω for two values of q. The frequencies for which $\mathrm{Im}\Pi_{21}$ vanishes represent regions for which single p-h excitations are forbidden. For $l_{\Delta_2} \to u_{\Delta_1}$ transition (rightmost curves of Fig. 3), the threshold behavior

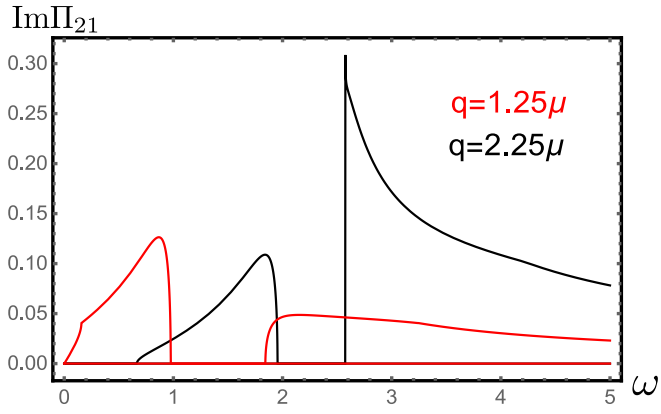

FIG. 3. Plotted are $\mathrm{Im}\Pi_{21}$ vs ω, where $\mathrm{Im}\Pi_{21}$ is obtained by adding the contributions $\mathrm{Im}\Pi_{21}^{uu}$ and $\mathrm{Im}\Pi_{21}^{lu}$. The two different q values lie in the range: $k_{F_1} - k_{F_2} < q = 1.25\mu < k_{F_1} + k_{F_2}$ and $k_{F_1} + k_{F_2} < q = 2.25\mu$. The corresponding q values are represented by the red and black dashed vertical lines in Fig. 2. Here and in subsequent plots ω and Π are in units of μ.

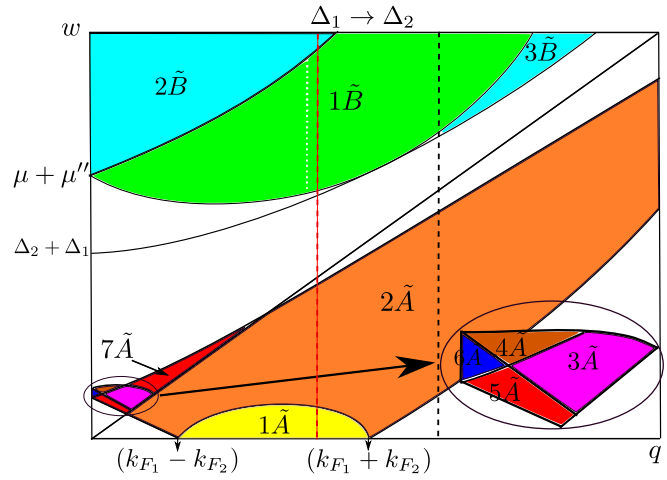

FIG. 4. Regions in the (q, ω) plane where $\Delta_1 \to \Delta_2$ transitions contribute to the imaginary part of the polarization function. $\tilde{\mathrm{A}}$ and $\tilde{\mathrm{B}}$ regions denote contributions from u_{Δ_1} to u_{Δ_2} and l_{Δ_1} to u_{Δ_2} transitions, respectively. Here $\mu'' = \sqrt{k_{F_2}^2 + \Delta_1^2}$.

exhibits contrasting features depending on whether q is lesser or greater than $(\Delta_s + \sqrt{\mu^2 - \Delta_2^2})/\Delta_1$ (the value at which $\omega = \sqrt{q^2 + \Delta_s^2}$ and $\omega = \mu + \sqrt{(q - k_{F_1})^2 + \Delta_2^2}$ curves intersect). For q values greater than $q^* = (\Delta_s + \sqrt{\mu^2 - \Delta_2^2})/\Delta_1$ the threshold behavior exhibits a step jump (shown by the black curve) to a finite value given by $q^2\Delta_1\Delta_2/\Delta_s^3$, whereas for lesser values of q it vanishes with the derivative acquiring a square-root singularity at $\omega = \mu + \sqrt{(q - k_{F_1})^2 + \Delta_2^2}$ (shown by the red curve). On the other hand, for u_{Δ_2} to u_{Δ_1} transition, the threshold behavior at the upper edge of region $2A$ vanishes, while the derivative diverges again with square-root singularity. Moreover, inside the allowed regions the plot exhibits a weak kink at various boundaries.

2. ($\Delta_1 \to \Delta_2$) *transition*

Similar to the earlier discussed upper band transitions, the transition from u_{Δ_1} to u_{Δ_2} are allowed for particles with energy ϵ in the range: $\max[\mu - \omega, \Delta_1] < \epsilon < \mu$. The major difference is that now the particle-hole transitions are allowed even for $\omega > q$ regions, albeit the phase space is much smaller than the phase space for the dominant $\omega < q$ regions [see the lower part of the (q, ω) plane in Fig. 4].

The maximum allowed frequency for such a transition is given by $\omega_{\max} = \max[\mu - \sqrt{(k_{F2} - q)^2 + \Delta_1^2}, \sqrt{(k_{F1} + q)^2 + \Delta_2^2} - \mu]$. The first term in the square bracket is the energy $\mu - \sqrt{(k_{F2} - q)^2 + \Delta_1^2}$ required for a collinear transition of a particle from u_{Δ_1} to the Fermi level of u_{Δ_2}. These transitions serve as the upper bound for frequency at small momentum transfer. The second frequency term $\sqrt{(k_{F1} + q)^2 + \Delta_2^2} - \mu$ is due to the collinear transition of a particle to u_{Δ_2} originating from the Fermi level of u_{Δ_1}. The lower bound of frequency for the u_{Δ_1} to u_{Δ_2} transition include $\sqrt{(k_{F1} - q)^2 + \Delta_2^2} - \mu$ (collinear transition from the Fermi level of the first band to the second band with the reduced momentum of the final particle) for momentum exchanges which lie between $0 < q < k_{F1} - k_{F2}$. In the range $k_{F1} - k_{F2} < q < k_{F1} + k_{F2}$ the transition can take place without change in the energy of the particle. While in the range $k_{F1} + k_{F2} < q$ the minimum energy required is $\sqrt{(k_{F1} - q)^2 + \Delta_2^2} - \mu$, which involves a transition from the Fermi level of the first band to a higher energy level of the second band with the final momentum reversing its direction.

The contribution to the imaginary part of the polarization function is as follows:

$$\mathrm{Im}\Pi_{12}^{uu}(q,\omega) = -\frac{1}{4\pi}\frac{1}{\sqrt{|q^2-\omega^2|}} \times \begin{Bmatrix} G_{12}^{uu}(2\mu+\omega\gamma_{12}) - G_{12}^{uu}(2\max[\mu-\omega,\Delta_1]+\omega\gamma_{12}) & :1\tilde{A} \\ G_{12}^{uu}(2\mu+\omega\gamma_{12}) - G_{12}^{uu}(\xi_{12}) & :2\tilde{A} \\ \bar{G}_{12}^{uu}(2\mu+\omega\gamma_{12}) - \bar{G}_{12}^{uu}(2\max[\mu-\omega,\Delta_1]+\omega\gamma_{12}) & :3\tilde{A} \\ \bar{G}_{12}^{uu}(\xi_{12}) - \bar{G}_{12}^{uu}(2\max[\mu-\omega,\Delta_1]+\omega\gamma_{12}) & :4\tilde{A} \\ \bar{G}_{12}^{uu}(2\mu+\omega\gamma_{12}) - \bar{G}_{12}^{uu}(-\xi_{12}) & :5\tilde{A} \\ \bar{G}_{12}^{uu}(\xi_{12}) - \bar{G}_{12}^{uu}(-\xi_{12}) & :6\tilde{A} \\ \bar{G}_{12}^{uu}(2\mu+\omega\gamma_{12}) - \bar{G}_{12}^{uu}(-\xi_{12}) & :7\tilde{A} \end{Bmatrix},$$

where $\gamma_{12} = 1 + \Delta_s\Delta_d/(q^2 - \omega^2)$, $\xi_{12} = \sqrt{q^2\gamma_{12}^2 + 4q^2\Delta_1^2/(q^2 - \omega^2)}$ and

$$G_{12}^{uu}(x) = \tfrac{1}{4}\{[-2q^2 - 2\Delta_d^2 + \xi_{12}^2 + 2(\omega\gamma_{12} - \omega)^2]\log\left(\sqrt{x^2 - \xi_{12}^2} + x\right) + [x - 4(\omega\gamma_{12} - \omega)]\sqrt{x^2 - \xi_{12}^2}\}, \quad (9)$$

$$\bar{G}^{uu}_{12}(x) = \frac{1}{4}\left\{\left[-2q^2 - 2\Delta_d^2 + \xi_{12}^2 + 2(\omega\gamma_{12} - \omega)^2\right]\tan^{-1}\left(\frac{x}{\sqrt{\xi_{12}^2 - x^2}}\right) - [x - 4(\omega\gamma_{12} - \omega)]\sqrt{\xi_{12}^2 - x^2}\right\}. \tag{10}$$

The different allowed regions in the (q, ω) plane for the u_{Δ_1} to u_{Δ_2} transition (Fig. 4) are as follows,

$$1\tilde{A} : \omega < \mu - \mathcal{F}(k_{F_2}, \Delta_1),$$
$$2\tilde{A} : \pm\mu \mp \mathcal{F}(k_{F_{2(1)}}, \Delta_{1(2)}) < \omega < -\mu + \mathcal{F}(-k_{F_1}, \Delta_2),$$
$$3\tilde{A} : \omega > q;\ \&\ \omega < \mu - \mathcal{F}(k_{F_2}, \Delta_1);\ \&\ \omega > \mu - \mathcal{F}(-k_{F_2}, \Delta_1);\ \&\ \omega < -\mu + \mathcal{F}(-k_{F_1}, \Delta_2),$$
$$4\tilde{A} : \omega > q;\ \&\ \omega < \mu - \mathcal{F}(k_{F_2}, \Delta_1);\ \&\ \omega > \mu - \mathcal{F}(-k_{F_2}, \Delta_1);\ \&\ \omega > -\mu + \mathcal{F}(-k_{F_1}, \Delta_2),$$
$$5\tilde{A} : \omega > q;\ \&\ \omega < -\mu + \mathcal{F}(-k_{F_1}, \Delta_2);\ \&\ \omega > -\mu + \mathcal{F}(k_{F_1}, \Delta_2);\ \&\ \omega < \mu - \mathcal{F}(-k_{F_2}, \Delta_1),$$
$$6\tilde{A} : \omega < \mu - \mathcal{F}(-k_{F_2}, \Delta_1);\ \&\ \omega > -\mu + \mathcal{F}(-k_{F_1}, \Delta_2),$$
$$7\tilde{A} : \omega > q;\ \&\ \omega > \mu - \mathcal{F}(k_{F_2}, \Delta_1);\ \&\ w < -\mu + \mathcal{F}(-k_{F_1}, \Delta_2),$$

A lower band l_{Δ_1} to upper band u_{Δ_2} transition requires the particle to have energy ϵ in the range: $\mu - \omega < \epsilon < -\Delta_1$. The derivation of the threshold frequencies is very similar as for the case of l_{Δ_2} to u_{Δ_1} transition and are obtained by simply exchanging the indices $1 \rightleftharpoons 2$. The threshold frequency for small q has the form $\omega = \mu + \sqrt{(k_{F_2} - q)^2 + \Delta_1^2}$ which changes to $\omega = \sqrt{q^2 + \Delta_s^2}$ at the point of intersection of the two curves. The contribution to the imaginary part of the polarization function is obtained to be:

$$\mathrm{Im}\Pi^{lu}_{12}(q, \omega) = -\frac{1}{4\pi}\frac{1}{\sqrt{\omega^2 - q^2}} \times \begin{Bmatrix} G^{lu}_{12}(2(\omega - \mu) - \omega\gamma_{12}) - G^{lu}_{12}(-\xi_{12}) & :1\tilde{B} \\ G^{lu}_{12}(\xi_{12}) - G^{lu}_{12}(-\xi_{12}) & :2\tilde{B} \\ G^{lu}_{12}(\xi_{12}) - G^{lu}_{12}(-\xi_{12}) & :3\tilde{B} \end{Bmatrix},$$

where,

$$G^{lu}_{12}(x) = \frac{1}{4}\left\{\left[2q^2 + 2\Delta_d^2 - \xi_{12}^2 - 2(\omega\gamma_{12} - \omega)^2\right]\tan^{-1}\left(\frac{x}{\sqrt{\xi_{12}^2 - x^2}}\right) + [x - 4(\omega\gamma_{12} - \omega)]\sqrt{\xi_{12}^2 - x^2}\right\}. \tag{11}$$

The nonzero regions in the (q, ω) plane (Fig. 4) are

$$1\tilde{B} : \mu + \mathcal{F}(k_{F_2}, \Delta_1) < \omega < \mu + \mathcal{F}(-k_{F_2}, \Delta_1)$$
$$2\tilde{B} : \omega > \mu + \mathcal{F}(-k_{F_2}, \Delta_1)$$
$$3\tilde{B} : \sqrt{q^2 + (\Delta_2 + \Delta_1)^2} < \omega < \mu + \mathcal{F}(k_{F_2}, \Delta_1).$$

Figure 5 shows $\mathrm{Im}\Pi_{12} = \mathrm{Im}\Pi^{uu}_{12} + \mathrm{Im}\Pi^{lu}_{12}$ plotted as a function of ω for three different values of q. The behavior for $l_{\Delta_1} \to u_{\Delta_2}$ (rightmost curves of Fig. 5) transition is similar to those considered in Fig. 3. In this case, the main change is in the position of q value given by $q^* = (\Delta_s + \sqrt{\mu^2 - \Delta_1^2})/\Delta_2$ which separates the two threshold behaviors. As before, for q values greater than it, the threshold behavior exhibits a step jump to the same finite value $q^2\Delta_1\Delta_2/\Delta_s^3$ (shown by the black curve), whereas for lesser q values the derivative at the threshold diverges (shown by the red curve). Also, for u_{Δ_1} to u_{Δ_2} transition, the threshold behavior at the upper edge vanishes everywhere, while the derivative diverges with square-root singularity. For the additional region shown in the inset, at small ω and $q < k_{F_1} - k_{F_2}$, the threshold behavior at both the edges exhibits square-root divergence of the derivatives. It turns out that in this region the real part of the polarization operator exhibits singular features, details of which are provided in Sec. V. Finally to conclude this section, $\mathrm{Im}\Pi_{xx/yy}$ is given by $\mathrm{Im}\Pi_{xx/yy} = \mathrm{Im}\Pi_{21} + \mathrm{Im}\Pi_{12}$. It is worth mentioning that in the absence of electric field $\Delta_1 = \Delta_2$, therefore $\mathrm{Im}\Pi_{12}$ and $\mathrm{Im}\Pi_{21}$ will be identical.

B. Imaginary part of χ_{zz}

For completeness we will discuss the result corresponding to the case of intra- and interband transitions within the same

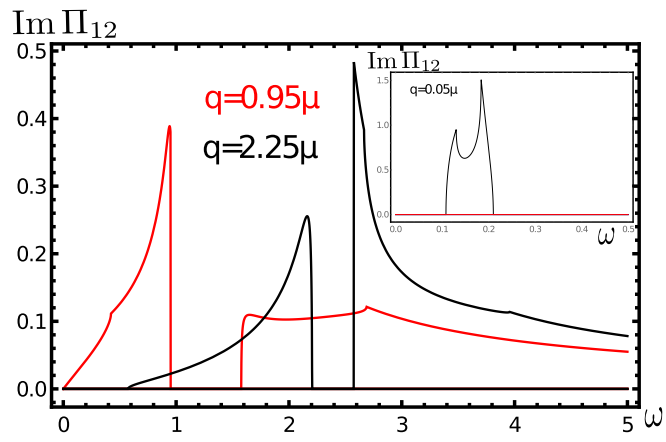

FIG. 5. Plotted are $\mathrm{Im}\Pi_{12}$ vs ω, where $\mathrm{Im}\Pi_{12} = \mathrm{Im}\Pi^{uu}_{12} + \mathrm{Im}\Pi^{lu}_{12}$. Here we have chosen q values to be $q = 0.95\mu$ and 2.25μ, and they lie in the following range: $k_{F_1} - k_{F_2} < 0.95\mu < k_{F_1} + k_{F_2}$ and $k_{F_1} + k_{F_2} < q = 2.25\mu$ (the q values are depicted by the red and black dashed vertical lines in Fig. 4, respectively). The features are very similar to those shown in Fig. 3, except here the discontinuities in the slopes are more pronounced. In the inset we plot for $q = 0.05\mu$, where $0.05\mu < k_{F_1} - k_{F_2}$; this additional feature is unique to $\Delta_1 \to \Delta_2$ transitions.

gap, i.e., $\Delta_i \to \Delta_i$ where $i \in \{1, 2\}$ (results can alternatively be obtained from the calculations of the charge susceptibility [31]). These give contributions to only $\mathrm{Im}\Pi_{zz}$ and as before they arise due to $u_{\Delta_i} \to u_{\Delta_i}$ and $l_{\Delta_i} \to u_{\Delta_i}$ transitions. The contribution to the imaginary part of the polarization function from the $u_{\Delta_i} \to u_{\Delta_i}$ transitions is as follows,

$$\mathrm{Im}\Pi^{uu}_{ii}(q,\omega) = -\frac{1}{4\pi}\frac{1}{\sqrt{q^2-\omega^2}} \times \begin{Bmatrix} G^{uu}(2\mu+\omega) - G^{uu}(2\max[\mu-\omega,\Delta_i]+\omega) & :1A' \\ G^{uu}(2\mu+\omega) - G^{uu}(\xi) & :2A' \end{Bmatrix},$$

$$\text{where} \quad \xi = \sqrt{q^2 + 4q^2\Delta_i^2/(q^2-\omega^2)}, \quad \text{and} \quad G^{uu}(x) = \tfrac{1}{4}\{[\xi^2 - 2q^2]\log(\sqrt{x^2-\xi^2}+x) + x\sqrt{x^2-\xi^2}\}. \tag{12}$$

The allowed regions for the transitions are (see Fig. 6)

$$1A' : \omega < \mu - \mathcal{F}(k_{F_i}, \Delta_i)$$
$$2A' : \pm\mu \mp \mathcal{F}(k_{F_i}, \Delta_i) < \omega < -\mu + \mathcal{F}(-k_{F_i}, \Delta_i).$$

Unlike the earlier two cases, the transitions within the same band allow the creation of particle-hole pairs having $\omega = 0$ and infinitesimally small momentum q.

The contribution from $l_{\Delta_i} \to u_{\Delta_i}$ transitions is

$$\mathrm{Im}\Pi^{lu}_{ii}(q,\omega) = -\frac{1}{4\pi}\frac{1}{\sqrt{\omega^2-q^2}} \times \begin{Bmatrix} G^{lu}(\omega-2\mu) - G^{lu}(-\xi) & :1B' \\ G^{lu}(\xi) - G^{lu}(-\xi) & :2B' \\ G^{lu}(\xi) - G^{lu}(-\xi) & :3B' \end{Bmatrix},$$

where

$$G^{lu}(x) = \frac{1}{4}\left[(2q^2-\xi^2)\tan^{-1}\left(\frac{x}{\sqrt{\xi^2-x^2}}\right) + x\sqrt{x^2-\xi^2}\right] \tag{13}$$

and the allowed regions in the (q, ω) plane are (see Fig. 6)

$$1B' : \mu + \mathcal{F}(k_{F_i}, \Delta_i) < \omega < \mu + \mathcal{F}(-k_{F_i}, \Delta_i)$$
$$2B' : \omega > \mu + \mathcal{F}(-k_{F_i}, \Delta_i)$$
$$3B' : \omega > (2k_{F_i}); \ \& \ \sqrt{q^2+(2\Delta_i)^2} < \omega < \mu + \mathcal{F}(k_{F_i}, \Delta_i).$$

Thus the K-valley contribution to $\mathrm{Im}\Pi_{zz}$ is given by $\sum_{i=1}^{2}(\mathrm{Im}\Pi^{lu}_{ii} + \mathrm{Im}\Pi^{uu}_{ii})$; identical contribution arises from the other valley. As an additional remark, we would like to point out that in the scenario of vanishing electric field, the zz component obtains identical contribution to xx/yy components.

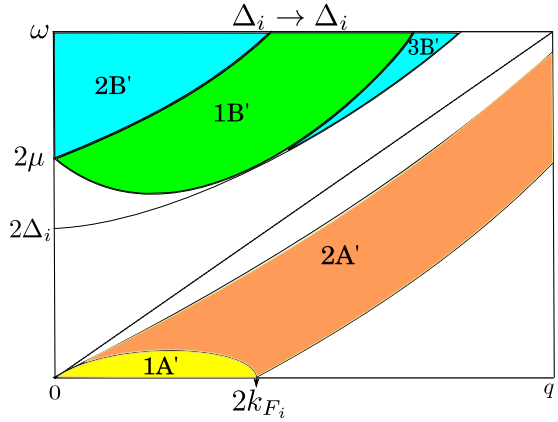

FIG. 6. The A′ regions denote contributions from $u_{\Delta_i} \to u_{\Delta_i}$, whereas B′ denote those from $l_{\Delta_i} \to u_{\Delta_i}$. Note $k_{F_i} = \sqrt{\mu^2 - \Delta_i^2}$.

V. REAL PART OF SPIN SUSCEPTIBILITY

The real part of spin susceptibility is evaluated from Eq. (5), where some of the parts have been calculated with the help of Kramers-Kronig technique and the rest via direct integration. The $\mathrm{Re}\chi_{xx}$ and $\mathrm{Re}\chi_{yy}$ are identical and obtain contributions from transitions involving $\Delta_1 \to \Delta_2$ and vice versa, while $\Delta_i \to \Delta_i$ $(i = 1, 2)$ transitions yield contributions to $\mathrm{Re}\chi_{zz}$. Details of the calculation are provided in the Appendix. In the following two subsections we will limit our discussion to the case of dynamic and static susceptibility.

A. Dynamic limit: $q = 0$

It is easy to show that for finite frequencies and $q = 0$, $\mathrm{Re}\chi_{zz}(q = 0, \omega)$ vanishes identically due to the Fermi-distribution terms in (5) (for $\alpha = \alpha'$) and form factor (6) (for $\alpha = -\alpha'$). In contrast, $\mathrm{Re}\chi_{xx}(0, \omega)$ and $\mathrm{Re}\chi_{yy}(0, \omega)$ are in general nonzero and exhibit interesting behavior in regions where the corresponding imaginary part vanishes. In the following, we will take a closer look into the different contributions to the real part of the susceptibility. As before, we will discuss the susceptibility in terms of the polarization operator which differs by a sign.

The noninteracting real part of the polarization operator (the xx and yy components) is split into three parts labeled as $\mathrm{Re}\Pi_a$, $\mathrm{Re}\Pi_b$, and $\mathrm{Re}\Pi_c$ (details of the decomposition and their derivation are given in Appendix 3). The first part, $\mathrm{Re}\Pi_a$, is independent of μ and takes on the value

$$\mathrm{Re}\,\Pi_a(\omega) = -\frac{\Delta_d^2}{4\pi\omega}\left\{\log\left[\frac{\Delta_s+\omega}{|\Delta_s-\omega|}\right]\left(1-\frac{\Delta_s^2}{\omega^2}\right) + \frac{2\Delta_s}{\omega}\right\},$$

where $\Delta_d = \Delta_2 - \Delta_1$ and $\Delta_s = \Delta_1 + \Delta_2$. The second term, $\mathrm{Re}\Pi_b$, is nonzero for $\mu > \Delta_1$ and obtains contribution from the integrals containing $n_F(\sqrt{p^2+\Delta_1^2}-\mu)$ and $n_F(\sqrt{(p+q)^2+\Delta_1^2}-\mu)$ terms and is given by

$$\mathrm{Re}\Pi_b(\omega) = -\frac{1}{4\pi}\left\{\frac{\Delta_d^2(\Delta_s^2-\omega^2)}{2\omega^3}\left(\log\left[\frac{(-\Delta_d\Delta_s-2\mu\omega+\omega^2)(-\Delta_d\Delta_s+2\omega\Delta_1+\omega^2)}{(-\Delta_d\Delta_s+2\mu\omega+\omega^2)(-\Delta_d\Delta_s-2\omega\Delta_1+\omega^2)}\right]\right) - \frac{2\Delta_d\Delta_s(\mu-\Delta_1)}{\omega^2}\right\}. \quad (14)$$

The third term denoted as $\mathrm{Re}\Pi_c$ obtains contribution from the integrals containing $n_F(\sqrt{p^2+\Delta_2^2}-\mu)$ and $n_F(\sqrt{(p+q)^2+\Delta_2^2}-\mu)$ terms and exhibits log divergence. It has the following form,

$$\mathrm{Re}\ \Pi_c(\omega) = -\frac{1}{4\pi}\left\{\frac{\Delta_d^2(\Delta_s^2-\omega^2)}{2\omega^3}\left(\log\left[\frac{(\Delta_d\Delta_s-2\mu\omega+\omega^2)(\Delta_d\Delta_s+2\omega\Delta_2+\omega^2)}{(\Delta_d\Delta_s+2\mu\omega+\omega^2)(\Delta_d\Delta_s-2\omega\Delta_2+\omega^2)}\right]\right) + \frac{2\Delta_d\Delta_s(\mu-\Delta_2)}{\omega^2}\right\}. \quad (15)$$

Combining all the contributions, $\mathrm{Re}\Pi(\omega) = \mathrm{Re}\Pi_a(\omega) + \mathrm{Re}\Pi_b(\omega) + \mathrm{Re}\Pi_c(\omega)$, we obtain the following compact expression,

$$\mathrm{Re}\Pi(\omega) = \frac{\Delta_d^2(\omega^2-\Delta_s^2)}{8\pi\omega^3}L(w), \quad (16)$$

where

$$L(w) = \log\left[\frac{(\omega^2-2\mu\omega)^2-\Delta_d^2\Delta_s^2}{(\omega^2+2\mu\omega)^2-\Delta_d^2\Delta_s^2}\right].$$

For $\omega > 0$, the real part of the susceptibility has singularities at the following four frequencies, $\omega = \sqrt{\mu^2 \pm \Delta_d\Delta_s}+\mu$, $\omega = \sqrt{\mu^2+\Delta_d\Delta_s}-\mu$, and $\omega = \mu - \sqrt{\mu^2-\Delta_d\Delta_s}$. Except for the frequency $\omega = \sqrt{\mu^2+\Delta_d\Delta_s}+\mu$ which is deep in the particle-hole excitation spectrum, the remaining three frequencies are exactly at the threshold of the particle-hole region, i.e., the imaginary part of the susceptibility vanishes in the regions $0 < \omega < \sqrt{\mu^2+\Delta_d\Delta_s}-\mu$ and $\mu - \sqrt{\mu^2-\Delta_d\Delta_s} < \omega < \sqrt{\mu^2-\Delta_d\Delta_s}+\mu$.

As will be discussed shortly, two of the singularities, one at $\omega_L = \sqrt{\mu^2+\Delta_d\Delta_s}-\mu$ and the other at $\omega_U = \sqrt{\mu^2-\Delta_d\Delta_s}+\mu$, are important from the point of view of spin-collective excitations. The origin of the log divergence at ω_L can be attributed specifically to the integral

$$I \propto \int \frac{pdp}{8\pi}\left[\left(1+\frac{p^2+\Delta_1\Delta_2}{\sqrt{p^2+\Delta_1^2}\sqrt{p^2+\Delta_2^2}}\right) \times \frac{\Theta\left(\sqrt{\mu^2-\Delta_1^2}-p\right)}{w+\sqrt{p^2+\Delta_1^2}-\sqrt{p^2+\Delta_2^2}}\right]. \quad (17)$$

Moreover, from the corresponding imaginary part of the integral it can be deduced that the processes responsible for the contribution involve upper-band transitions from $u_{\Delta_1} \to u_{\Delta_2}$ (see Fig. 7). Similarly, the log divergence at ω_U (corresponding to the upper threshold for the single particle excitation) is due to the integral

$$I \propto \int \frac{pdp}{8\pi}\left[\left(1-\frac{p^2+\Delta_1\Delta_2}{\sqrt{p^2+\Delta_1^2}\sqrt{p^2+\Delta_2^2}}\right) \times \frac{\Theta\left(\sqrt{\mu^2-\Delta_2^2}-p\right)}{w-\sqrt{p^2+\Delta_1^2}-\sqrt{p^2+\Delta_2^2}}\right], \quad (18)$$

where the contributions again arise from $\Delta_1 \to \Delta_2$ transition, however, l_{Δ_1} and u_{Δ_2} now correspond to the lower and upper bands, respectively.

Turning on weak electron-electron interaction by including the Hubbard term $V = u^* \int dx \rho_\uparrow \rho_\downarrow$ yields perturbative corrections to the susceptibility for all frequencies, except near the frequencies corresponding to log singularities. At the nth order in interaction, the ladder diagram contributes the strongest singularity with $(n+1)$th power of the original log singularity. Therefore, the susceptibility for frequencies near the log singularities is described by taking into consideration interactions to all orders. This entails summing up the ladder series of the diagram yielding a modified form for the spin susceptibility. Similar to approaches obtained within the framework of a molecular field or random phase approximation (RPA), this implies the spin susceptibility gets renormalized by the term $1/(1+u\chi(\omega))$ [55,56]. Interestingly, for frequencies slightly lower than ω_U and ω_L, $\chi(\omega)$ is purely real and

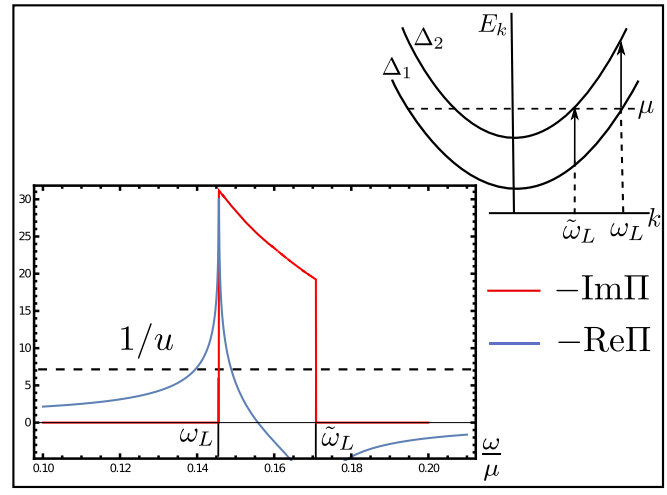

FIG. 7. The dotted line denotes $1/u$, while the blue curve represents $-\mathrm{Re}\Pi(\omega)$. The collective excitation pole (near the lower threshold) is given by the frequency at which they intersect. The red line corresponds to the imaginary part of the polarization function, where its boundaries are $\omega_L = \sqrt{\mu^2-\Delta_1^2+\Delta_2^2}-\mu$ and $\tilde{\omega}_L = \mu - \sqrt{\mu^2+\Delta_1^2-\Delta_2^2}$.

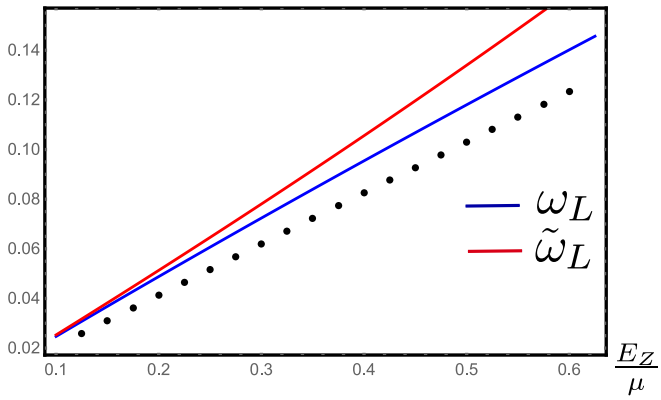

FIG. 8. The dashed-dotted line denotes the pole position as a function of perpendicular electric field E_Z for fixed interaction $u = 0.5$, while the blue and red solid curves correspond to the behavior of two lower threshold frequency ω_L and $\tilde{\omega}_L$ with electric field, where in between the imaginary part of polarization function is nonzero.

negative. This, coupled with the presence of log singularity at ω_U and ω_L implies that a pole structure develops (irrespective of how weak the interaction might be), the solution of which corresponds to the spin-collective excitation frequency.

Solving the pole equations yields two solutions close to the threshold frequencies (see Fig. 7 for solution near the lower threshold) given by

$$\omega_1 = \omega_L - \frac{2\mu(\mu'-\mu)(\mu'-\mu''-2\mu)(\mu'+\mu''-2\mu)}{\mu'(\mu'-\mu'')(\mu'+\mu'')} \times \exp\left[\frac{8\pi(\mu'-\mu)^3}{u\left[(\mu'-\mu)^2-\Delta_s^2\right]\Delta_d}\right], \tag{19}$$

and a solution just below the upper threshold,

$$\omega_2 = \omega_U - \frac{2\mu(\mu+\mu'')(\mu'-\mu''-2\mu)(\mu'+\mu''+2\mu)}{\mu''(\mu'-\mu'')(\mu'+\mu'')} \times \exp\left[\frac{8\pi(\mu'-\mu)^3}{u\left[(\mu'-\mu)^2-\Delta_s^2\right]\Delta_d}\right], \tag{20}$$

where $\mu' = \sqrt{\mu^2+\Delta_d\Delta_s}$ and $\mu'' = \sqrt{\mu^2-\Delta_d\Delta_s}$. We note that in the absence of external electric field the two gaps Δ_1 and Δ_2 are identical, therefore the $\mathrm{Re}\Pi(\omega)$ vanishes identically and no pole solutions are possible. In Fig. 8 we show the explicit dependence of the threshold frequencies ω_L and $\tilde{\omega}_L$ and the lower pole position on the perpendicular electric field E_Z. For nonzero electric field, the slope of ω_L and $\tilde{\omega}_L$ are $2E_Z/\sqrt{\mu^2 \pm 4E_Z\lambda_{SO}}$, respectively, therefore the width of the real region given by $\tilde{\omega}_L - \omega_L$ grows wider with increasing electric field. At the same time the slope of pole position for a fixed interaction u is even lesser than the slope of ω_L therefore the width between the pole position and ω_L also increases.

While the above discussion hints at the possibility of collective excitations it turns out that the presence of the sublattice degrees of freedom complicates the analysis. The pole equation has its structure modified due to the presence of τ_i type of terms in the Green's function. Even though Π_{xx} has only σ_x on either ends of the polarization bubble, the vertex corrected (due to electron-electron interactions) spin susceptibility acquires contributions from all τ_i's. For example, the lowest order vertex term $\propto u\int \hat{G}_{P+Q}\sigma_x\hat{G}_P$ has τ dependence arising due to the Green's function. In terms of the vertex term Λ the interacting susceptibility, Π_{xx}^{int}, is given by

$$\Pi_{xx}^{\mathrm{int}} = \int_P \mathrm{Tr}\left[\sigma_x\hat{G}_P\Lambda_x^0\hat{G}_{P+Q}\right], \tag{21}$$

where Λ satisfies the equation:

$$\Lambda_j^\beta = \sigma_j\tau_\beta - u\int \hat{G}_P\Lambda_j^\beta\hat{G}_{P+Q}, \tag{22}$$

where we will use $\{1, 2, 3\}$ interchangeably for $\{x, y, z\}$. For the Hubbard-type interaction, Λ will be a function of Q only and can be expressed as a linear combination of $\sigma_k\tau_\gamma$ (where $k, \gamma = 0\cdot\cdot 3$) [39]. We express Λ_j^β as

$$\Lambda_j^\beta = \sigma_k\tau_\gamma M_{[4j+\beta]}^{[4k+\gamma]}, \tag{23}$$

(where there is a summation on k and γ indices and the 16×16 matrix M is a function of only Q) in Eq. (22) and obtain

$$\left(\sigma_k\tau_\gamma + u\int \hat{G}_P\sigma_k\tau_\gamma\hat{G}_{P+Q}\right)M_{[4j+\beta]}^{[4k+\gamma]} = \sigma_j\tau_\beta. \tag{24}$$

Multiplying both sides of Eq. (24) with $\sigma_m\tau_\nu$ and taking the trace yields

$$(\delta_{m,k}\delta_{\nu,\gamma} + \frac{u}{4}\tilde{\Pi}_{[4k+\gamma]}^{[4m+\nu]})M_{[4j+\beta]}^{[4k+\gamma]} = \delta_{m,j}\delta_{\nu,\beta}, \tag{25}$$

where $\tilde{\Pi}$ is the generalized noninteracting susceptibility matrix whose elements are defined as $\tilde{\Pi}_{[4j+\beta]}^{[4m+\nu]} = \mathrm{Tr}[\int_P \sigma_m\tau_\nu\hat{G}_P\sigma_j\tau_\beta\hat{G}_{P+Q}]$. The matrix M derived from Eqs. (24) and (25) is given by $M = (I + u\tilde{\Pi}/4)^{-1}$. Thus Π_{xx}^{int} acquires the form

$$\Pi_{xx}^{\mathrm{int}} = \int_P \mathrm{Tr}\left[\sigma_x\hat{G}_P\sigma_k\tau_\gamma M_{[4]}^{[4k+\gamma]}\hat{G}_{P+Q}\right]. \tag{26}$$

We find that many of the elements of $\tilde{\Pi}(\omega)$ matrix exhibit ultraviolet divergence. We will illustrate one such example; consider the $\tilde{\Pi}_{55}$ element given by $\tilde{\Pi}_{55}(\omega) = \mathrm{Tr}[\int_P \sigma_1\tau_1\hat{G}_P\sigma_1\tau_1\hat{G}_{P+Q}]$. Here the terms independent of the chemical potential, i.e.,

$$I_\pm \propto \int pdp\left(1 + \frac{\Delta_1\Delta_2}{E_1(p)E_2(p)}\right)\frac{1}{E_1(p)+E_2(p)\pm\omega}, \tag{27}$$

obtain divergent contributions from the upper limit due to the Dirac spectrum and necessitate one to consider nonlinear terms arising from the exact energy spectrum. The divergence of Eq. (16) is expected to be altered in the interacting version $\Pi_{xx}^{\mathrm{int}} = \int_P \mathrm{Tr}[\sigma_x\hat{G}_P\Lambda_x^0\hat{G}_{P+Q}]$, however, we expect the collective excitations to survive.

B. Static limit: $\omega = 0$

Following earlier discussion, the components of spin susceptibility that yield nonvanishing contributions are $\mathrm{Re}\Pi_{zz}$ and $\mathrm{Re}\Pi_{xx/yy}$. $\mathrm{Re}\Pi_{zz}$ can be conveniently decomposed into the sum of $\mathrm{Re}\Pi_{zz-1} + \mathrm{Re}\Pi_{zz-2}$ which are the contributions from transitions involving $\Delta_i \to \Delta_i (i = 1, 2)$. For $q < 2k_{F_i}$,

$\mathrm{Re}\Pi_{zz-i}$ is a constant. Subtracting the constant part we obtain

$$\delta\mathrm{Re}\Pi_{zz-i} = \left[\frac{\mu\sqrt{q^2-\left(2k_{F_i}\right)^2}}{4\pi q} - \frac{\left(q^2-4\Delta_i^2\right)}{8\pi q} \times \tan^{-1}\left(\frac{\sqrt{q^2-\left(2k_{F_i}\right)^2}}{2\mu}\right)\right]\Theta\left(q-2k_{F_i}\right). \quad (28)$$

The above expression is identical to the charge susceptibility case [20,31,32,52,54]. For large distances the zz component of the spin susceptibility is given by

$$\chi_{zz-i}(r) \sim \int \mathrm{d}q\sqrt{q}\frac{\cos(rq-\pi/4)}{\sqrt{r}}\delta\Pi_{zz-i}(q). \quad (29)$$

Taking into consideration that the first derivative of $\mathrm{Re}\Pi_{zz-i}$ diverges at $2k_{F_i}$ as

$$\mathrm{Re}\delta\Pi'_{zz-i} \approx \frac{\Delta_i^2}{\pi\mu\sqrt{2k_{F_i}}}\frac{1}{\sqrt{q-2k_{F_i}}}, \quad (30)$$

the integral reduces to

$$\chi_i(r) \sim \int dq\frac{\sqrt{q}\sin(rq-\pi/4)}{r^{3/2}\sqrt{q-2k_{F_i}}}. \quad (31)$$

Thus one can deduce from simple power counting arguments that at large distances the zz component of the spin-susceptibility decays as $1/r^2$ and the contribution to exchange interaction is oscillatory with two wavelengths given by π/k_{F_1} and π/k_{F_2}. For electric field strength equal to $E_z^c = \lambda_{SO}/l$, $\Delta_1 = 0$ and therefore the first derivative of $\mathrm{Re}\Pi_{zz-1}$ vanishes. It is the second derivative which diverges at $2k_{F_1}$ as $\mathrm{Re}\Pi''_{zz-1} \approx -(1/8\pi\sqrt{k_{F_i}})/\sqrt{q-2k_{F_i}}$ that determines the long distance behavior of $\mathrm{Re}\chi_{zz-1}$. The susceptibility now acquires a faster $1/r^3$ decay. For $\mu > \Delta_2$ this behavior will be masked by the slower $1/r^2$ decay arising due to $\mathrm{Re}\chi_{zz-2}$, however for $\mu < \Delta_2$, only the $1/r^3$ term will survive.

Next consider the behavior of $\mathrm{Re}\Pi_{xx/yy}$ (details of the derivation are given in Appendix 2). The terms which are independent of the chemical potential yield regular contributions for all values of q given by

$$\mathrm{Re}\,\Pi_a(q) = -\frac{\Delta_d^2+q^2}{4\pi q^3}\left\{\left[q^2-\Delta_s^2\right]\tan^{-1}\left(\frac{q}{\Delta_s}\right)+q\Delta_s\right\}. \quad (32)$$

While from the integrals containing $n_F(\sqrt{p^2+\Delta_1^2}-\mu)$ we obtain

$$\mathrm{Re}\Pi_b(q) = \left\{\begin{array}{ll} -\frac{\mu-\Delta_1}{2\pi} - \frac{\mathrm{sgn}\left(q^2+\Delta_2^2-\Delta_1^2\right)}{4\pi q}[Y(\mu)-Y(\Delta_1)], & \text{for } q < k_{F_1}-k_{F_2} \text{ or } q > k_{F_1}+k_{F_2}, \\ -\frac{\mu-\Delta_1}{2\pi} - \frac{\mathrm{sgn}\left(q^2+\Delta_2^2-\Delta_1^2\right)}{4\pi q}[Y(\xi)-Y(\Delta_1)], & \text{for } k_{F_1}-k_{F_2} < q < k_{F_1}+k_{F_2}, \end{array}\right\} \quad (33)$$

where

$$Y(x) = \left\{-2x\sqrt{\xi^2-x^2} - \tan^{-1}\left(\frac{x}{\sqrt{\xi^2-x^2}}\right)\left[q^2-2\xi^2+\Delta_d^2\right]\right\}. \quad (34)$$

The remaining term arising from the integrals containing $n_F(\sqrt{p^2+\Delta_2^2}-\mu)$ denoted by $\mathrm{Re}\Pi_c(q)$ is obtained by simply changing Δ_1 to Δ_2 and vice versa in Eq. (33). The derivatives of both $\mathrm{Re}\Pi_b(q)$ and $\mathrm{Re}\Pi_c(q)$ diverge at $q_d = k_{F_1}-k_{F_2}$ and $q_s = k_{F_1}+k_{F_2}$ (see Fig. 9). However, combining them together we find that the divergence at q_d is canceled and that $\mathrm{Re}\Pi_{xx/yy}$ is constant for $q < q_s$, while the divergence at q_s remains. Removing the constant part, the full expression for the static susceptibility is given by

$$\delta\mathrm{Re}\Pi_{xx/yy}(q) = \left[\frac{\mu\sqrt{\left(q^2-q_s^2\right)\left(q^2-q_d^2\right)}}{2\pi q^2} - \frac{\left(q^2+\Delta_d^2\right)\left(q^2-\Delta_s^2\right)}{4\pi q^3}\tan^{-1}\left(\frac{\sqrt{\left(q^2-q_s^2\right)\left(q^2-q_d^2\right)}}{2\mu q}\right)\right]\Theta(q-k_{F_1}-k_{F_2}).$$

The derivative of the polarization operator has a square-root singularity at $q = q_s$ given by

$$\delta\mathrm{Re}\Pi'_{xx/yy}(q) \approx -\frac{\sqrt{k_{F_1}k_{F_2}}\left[\left(q^2+\Delta_d^2\right)\left(q^2-\Delta_s^2\right)-4\mu^2q_s^2\right]}{4\sqrt{2}\pi\mu q_s^{7/2}\sqrt{q-q_s}},$$

therefore the real space decay exhibits $1/r^2$ power-law dependence at large distances while the oscillatory wavelength is now given by $2\pi/q_s = 2\pi/(k_{F_1}+k_{F_2})$. Rather interestingly, for the xx and yy parts of the spin susceptibility, unless both the gaps are equal ($\Delta_1 = \Delta_2$), closing of one of the gaps does not lead to vanishing of the singular behavior of the derivative at $k_{F_1}+k_{F_2}$. Thus the $1/r^2$ power-law dependence at large distances is maintained irrespective of the tuning of the gaps by the electric field.

The real space analysis thus far yields the behavior of spin-spin correlation function between spins that are widely separated from each other and are delocalized on few sites. The calculation of spin correlations thus entails disregarding intervalley scattering and taking the trace of the sublattice degrees of freedom. In contrast, the behavior of spin correlations between two impurity spins that are localized on specific sites of the lattice is given by a different version of static spin susceptibility that also yields the Ruderman-Kittel-Kasuya-Yosida (RKKY) interaction between the two localized spins (see [42,57] for a detailed analysis for the case of silicene). Due to the short-range nature of interactions between the localized impurities and itinerant electrons, an intervalley scattering of the electrons via large $2K$ momentum exchange is allowed leading to additional contributions to

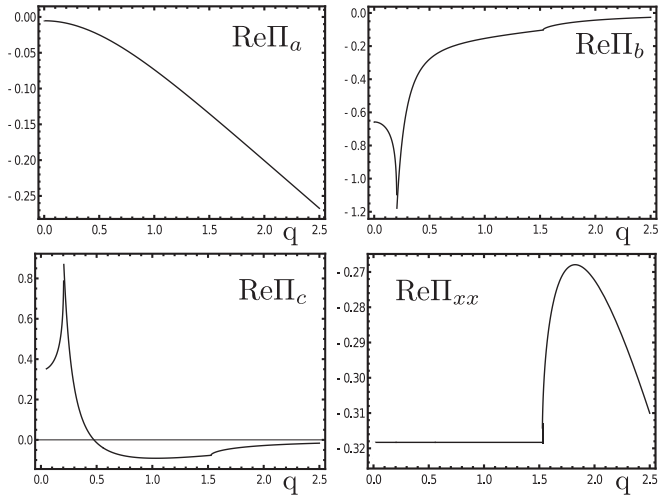

FIG. 9. Here we consider the contributions to $\mathrm{Re}\Pi_{xx/yy}(q,\omega=0)$. As in Appendix 2, we split the full integral into $\mathrm{Re}\Pi_a$, $\mathrm{Re}\Pi_b$, and $\mathrm{Re}\Pi_c$ and examine their behavior. The contribution from $\mathrm{Re}\Pi_a$ is smooth and continuous. The sharp features of $\mathrm{Re}\Pi_b$ and $\mathrm{Re}\Pi_c$ at $k_{F_1}-k_{F_2}$ come with opposite sign, however, the kinklike features at $k_{F_1}+k_{F_2}$ have the same sign and when all three contributions are combined the features at $k_{F_1}+k_{F_2}$ are enhanced while those at $k_{F_1}-k_{F_2}$ cancel exactly.

the spin susceptibility. Moreover, the position of the spin impurities (whether the two spins are on A-A/B-B sites or A-B sites) also crucially determines the behavior of spin correlations. In what follows, we will briefly discuss the differences and similarities between the results arising from these two different scenarios.

The effective interaction between two magnetic impurities $\vec{S}_i$ and $\vec{S}_j$ (localized at sites $\vec{R}_i$ and $\vec{R}_j$, respectively) is given by $H_{\mathrm{RKKY}}=-J^2\chi^{cd}_{\alpha\beta}S^\alpha_i S^\beta_j$ [41,58], where there is a repeated summation on only the spin indices $\alpha,\beta=x,y,z$; the indices c, d refer to the A or B sites and J is the interaction term between the magnetic impurity and itinerant electrons. The spin-susceptibility matrix has the form

$$\chi_{\alpha,\beta}(R_{ij})=\frac{1}{\hbar}\int_0^\infty \mathrm{Tr}[\sigma_\alpha\mathcal{G}(i,j;\tau)\sigma_\beta\mathcal{G}(j,i;-\tau)]d\tau, \tag{35}$$

where the trace is only over the spin degrees of freedom [41,58]. The Green's function is a 4×4 matrix,

$$\mathcal{G}(i,j;\pm\tau)=\mp\sum_n \psi_n(j)\psi_n^\dagger(i)e^{\mp\tilde{\epsilon}_n\tau}\Theta(\pm\tilde{\epsilon}_n), \tag{36}$$

where $n\in\{\eta,p,s\}$ is a summation on valley, momentum, and spin degrees of freedom, $\tilde{\epsilon}_n=\epsilon_n-\mu$, and the wave functions in the basis $\psi_n=(\psi_{A\uparrow},\psi_{B\uparrow},\psi_{A\downarrow},\psi_{B\downarrow})^T$ are given by

$$\psi_{(\eta,p,\uparrow)}=\frac{e^{i(\eta K+p)R_i}}{\sqrt{2\epsilon_{\eta\uparrow}(\epsilon_{\eta\uparrow}+\nu\Delta_{\eta\uparrow})}}\begin{bmatrix} pe^{-i\eta\theta}\\ \nu\epsilon_{\eta\uparrow}+\Delta_{\eta\uparrow}\\ 0\\ 0\end{bmatrix}, \tag{37}$$

and

$$\psi_{(\eta,p,\downarrow)}=\frac{e^{i(\eta K+p)R_i}}{\sqrt{2\epsilon_{\eta\downarrow}(\epsilon_{\eta\downarrow}+\nu\Delta_{\eta\downarrow})}}\begin{bmatrix} 0\\ 0\\ pe^{-i\eta\theta}\\ \nu\epsilon_{\eta\downarrow}+\Delta_{\eta\downarrow}\end{bmatrix}, \tag{38}$$

where $\nu=\pm1$ represents conduction/valence band, respectively.

Let us for example consider χ^{AA}_{xx} and χ^{AA}_{xy} which are obtained from the following integrals

$$\chi^{\mathrm{AA}}_{xx}=\int_0^\infty\left(g^{\mathrm{AA}}_{\uparrow\uparrow}\bar{g}^{\mathrm{AA}}_{\downarrow\downarrow}+g^{\mathrm{AA}}_{\downarrow\downarrow}\bar{g}^{\mathrm{AA}}_{\uparrow\uparrow}\right)d\tau/\hbar \tag{39}$$

and

$$\chi^{\mathrm{AA}}_{xy}=-i\int_0^\infty\left(g^{\mathrm{AA}}_{\uparrow\uparrow}\bar{g}^{\mathrm{AA}}_{\downarrow\downarrow}-g^{\mathrm{AA}}_{\downarrow\downarrow}\bar{g}^{\mathrm{AA}}_{\uparrow\uparrow}\right)d\tau/\hbar, \tag{40}$$

where $g^{\mathrm{AA}}_{ss}=e^{\mu\tau}\sum_\eta e^{i\eta\vec{K}.\vec{R}_{ij}}\mathcal{A}_{\eta,s}$ and

$$\mathcal{A}_{\eta,s}=-\frac{a^2}{4\pi}\int\frac{p^3dp\Theta(\epsilon_{\eta s}-\mu)}{\epsilon_{\eta s}(\epsilon_{\eta s}+\Delta_{\eta s})}J_0(p|\vec{R}_{ij}|)e^{-\epsilon_{\eta s}\tau}. \tag{41}$$

Similarly $\bar{g}^{\mathrm{AA}}_{ss}=e^{-\mu\tau}\sum_\eta e^{-i\eta\vec{K}.\vec{R}_{ij}}\bar{\mathcal{A}}_{\eta,s}$, where

$$\bar{\mathcal{A}}_{\eta,s}=\frac{a^2}{4\pi}\int\sum_\nu\frac{p^3dp\Theta(\mu-\nu\epsilon_{\eta s})}{\epsilon_{\eta s}(\epsilon_{\eta s}+\nu\Delta_{\eta s})}J_0(p|\vec{R}_{ij}|)e^{\nu\epsilon_{\eta s}\tau}.$$

Taking the product

$$g^{\mathrm{AA}}_{\uparrow\uparrow}\bar{g}^{\mathrm{AA}}_{\downarrow\downarrow}=\sum_{\eta,\eta'}e^{i(\eta-\eta')\vec{K}.\vec{R}_{ij}}\mathcal{A}_{\eta,\uparrow}\bar{\mathcal{A}}_{\eta',\downarrow}, \tag{42}$$

and

$$g^{\mathrm{AA}}_{\downarrow\downarrow}\bar{g}^{\mathrm{AA}}_{\uparrow\uparrow}=\sum_{\eta,\eta'}e^{i(\eta-\eta')\vec{K}.\vec{R}_{ij}}\mathcal{A}_{\eta,\downarrow}\bar{\mathcal{A}}_{\eta',\uparrow}, \tag{43}$$

we identify that the contributions can be classified into intra- ($\eta=\eta'$) and intervalley ($\eta=-\eta'$) terms. While for χ^{AA}_{xx} the intraterms add up, they cancel identically for χ^{AA}_{xy}. Similar cancellation holds for χ^{AB}_{xy}. This result is consistent with our earlier result (which takes into consideration only the intraterms) regarding the vanishing of χ_{xy} term when contributions from the valleys are added together. However due to the intervalley scattering processes, χ^{AB}_{xy} and χ^{AA}_{xy} obtain additional nonvanishing contributions. Another important difference is that, besides the oscillatory dependence with wave number $2\pi/(k_{F_1}+k_{F_2})$ due to the intravalley process, the intervalley processes yield additional oscillatory dependence on $\vec{R}$ arising from terms of the type $e^{i2\eta\vec{K}.\vec{R}_{ij}}\mathcal{A}_{\eta,\uparrow}\bar{\mathcal{A}}_{-\eta,\downarrow}$ [see Eq. (42)].

VI. SUMMARY

In this paper, we have presented a detailed study of the spin susceptibility for silicene that can be generalized to other buckled honeycomb structured materials, e.g., germanene and stanene which also exhibit an electric field tunable band gap. We find that the simultaneous presence of the inversion symmetric Kane-Mele mass term $\hat{\sigma}_z\otimes\hat{\tau}_z$ and the inversion symmetry breaking electric field term $\hat{I}\otimes\hat{\tau}_z$ are responsible for features in the spin susceptibility which are otherwise

absent even if one of the terms is turned off. The two terms conspire to break the band degeneracy at each of the valleys and therefore, while the xx and yy components of the spin susceptibility are identical, the zz component is different. The xx and yy components obtain contributions from only those electronic transitions for which the spins are flipped, while the zz component obtains contributions from spin conserving processes. Although the off-diagonal components of the spin susceptibility, $0z$ and xy, are nonzero in individual valleys, adding the contributions from the valleys leads to cancellation.

The study of the imaginary part of spin susceptibility reveals regions in the (q, ω) plane where the single-particle excitations are allowed. We find that the threshold behavior for the lower- to upper-band transition is especially interesting since its behavior changes upon increasing the value of q. For q values smaller than a special momentum q^* (as defined in the main text) the threshold behavior exhibits a square-root singularity in its derivative, whereas for $q > q^*$ the susceptibility acquires a finite jump. We have investigated the role of electric field E_Z in extending the allowed regions for particle-hole transitions. Electric field is also responsible for yielding differing contributions for the $\Delta_1 \to \Delta_2$ transitions as compared to those from the $\Delta_2 \to \Delta_1$ transitions.

We have studied the real part of spin susceptibility, with particular emphasis on the dynamic and static limits. In the dynamic limit, we show that the real part of spin susceptibility exhibits log divergence. The origin of divergence at low frequencies can be traced to the $u_{\Delta_1} \to u_{\Delta_2}$ transitions, whereas those at high frequencies can be attributed to $l_{\Delta_1} \to u_{\Delta_2}$ transitions. We explore the significance of the divergence for spin-collective excitations and the dependence of the excitations on the external electric field. Interestingly, these excitations are absent if either the spin-orbit term or the electric field term is absent.

The study of the static part of the spin susceptibility reveals Kohn anomaly at $k_{F_1} + k_{F_2}$ for the xx/yy components of the spin susceptibility, whereas for the zz component the anomaly is present at $2k_{F_1}$ and $2k_{F_2}$. At generic electric field strengths the first derivative of the spin susceptibility has a square root singularity, consequently, the long-distance signature of the Kohn anomaly is revealed as $1/r^2$ decay of the spin susceptibility. However, when the field strength is tuned to E_z^c, the gap Δ_1 vanishes leading to a rather dramatic effect on the behavior of the spin susceptibility in the zz channel. The Kohn anomaly at $2k_{F1}$ is modified and results in a $1/r^3$ decay in the spin susceptibility. This decay feature becomes prominent when the chemical potential is in between the Δ_1 and Δ_2 gap.

ACKNOWLEDGMENTS

We would like to thank S. Dutta, A. K. Sorout, and V. Zyuzin for useful discussions. We thank the anonymous referees for constructive comments and suggestions. S.G. is grateful to SERB for the support via the Grant No. EMR/2016/002646.

APPENDIX

1. Derivation of Re $\Pi_{xx/yy}(\mathbf{q}, \omega)$

We will integrate the terms of Eq. (5) by first obtaining the contribution from $\Delta_1 \to \Delta_2$ transition by taking $\beta = +1$ and $\beta' = -1$ (for all possible values of α, α' for the K valley). We divide the real part of polarization operator $\Pi(q, w)$ as follows,

$$A_1 = -\frac{1}{2}\int \frac{d^2p}{(2\pi)^2}\left(1 + \frac{\vec{p}_1 \cdot (\vec{p}+\vec{q})_2}{E_1(p)\cdot E_2(p+q)}\right)\left[\frac{n_F[E_1(p)]}{-E_1(p)+E_2(p+q)-\omega} - \frac{n_F[E_2(p+q)]}{-E_1(p)+E_2(p+q)-\omega}\right]$$

$$A_2 = -\frac{1}{2}\int \frac{d^2p}{(2\pi)^2}\left(1 - \frac{\vec{p}_1 \cdot (\vec{p}+\vec{q})_2}{E_1(p)\cdot E_2(p+q)}\right)\left[\frac{1}{+E_1(p)+E_2(p+q)-\omega} - \frac{n_F[E_2(p+q)]}{+E_1(p)+E_2(p+q)-\omega}\right]$$

$$A_3 = -\frac{1}{2}\int \frac{d^2p}{(2\pi)^2}\left(1 - \frac{\vec{p}_1 \cdot (\vec{p}+\vec{q})_2}{E_1(p)\cdot E_2(p+q)}\right)\left[\frac{n_F[E_1(p)]}{-E_1(p)-E_2(p+q)-\omega} - \frac{1}{-E_1(p)-E_2(p+q)-\omega}\right],$$

where $F^{1,-1}_{xx/yy} = 2$, $\vec{p}_{1/2} = p_x\hat{e}_1 + \eta p_y \hat{e}_2 + \Delta_{1/2}\hat{e}_3$, $\quad E_1(p) = \sqrt{p^2+\Delta_1^2}$, and $E_2(p) = \sqrt{p^2+\Delta_2^2}$.

The first term of A_2 and the second term of A_3 yield terms that are independent of μ; we combine them together and represent it as Π_{12-a}. ImΠ_{12-a} is given by

$$\mathrm{Im}\,\Pi_{12-a}(q,\omega) = -\tfrac{1}{16}\Theta\big(\omega^2 - q^2 - \Delta_s^2\big)\mathrm{Y}(q,\omega), \tag{A1}$$

where

$$\mathrm{Y}(q,\omega) = \frac{1}{\sqrt{\omega^2-q^2}}\left\{\left[q^2+2\Delta_d^2\right] + \left[\frac{2q^2\big(\Delta_1^2+\Delta_2^2\big) - 2(\Delta_s\Delta_d)^2}{\omega^2-q^2}\right] - \left[\frac{3q^2(\Delta_s\Delta_d)^2}{(\omega^2-q^2)^2}\right]\right\}. \tag{A2}$$

We use the above result to calculate ReΠ_{12-a} via the Kramers-Kronig relation:

$$\begin{aligned}\mathrm{Re}\,\Pi_{12-a}(q,\omega) &= \frac{1}{\pi}\mathrm{P}\int_{-\infty}^{\infty} d\omega' \frac{\mathrm{Im}\,\Pi_{12-a}(q,\omega')}{(\omega'-\omega)}\,\mathrm{sgn}(\omega') = -\frac{1}{16\pi}\mathrm{P}\left(\int_{\gamma}^{\infty} d\omega' \frac{\mathrm{Y}(q,\omega')}{(\omega'-\omega)} - \int_{-\infty}^{-\gamma} d\omega' \frac{\mathrm{Y}(q,\omega')}{(\omega'-\omega)}\right)\\ &= -\frac{1}{16\pi}(\Theta(q-\omega)f(q,\omega) + \Theta(\omega-q)g(q,\omega)).\end{aligned} \tag{A3}$$

The first integral is performed with the aid of the following variable change ω' to x, where they are related via $\omega'=q(1+x^2)/(1-x^2)$. Similar transformation is used for the second integral.

For $q > \omega$, the result of the integration is $f(q,\omega)$ which is expressed as a sum of three parts, $f(q,\omega) = f_1(q,\omega) + f_2(q,\omega) + f_3(q,\omega)$ [corresponding to the square brackets of $Y(q,\omega)$] and they are given by

$$f_1(q,\omega) = \left(q^2+2\Delta_d^2\right)\left\{\frac{2}{(q+\omega)}\left[\frac{1}{\tilde{\beta}_1}\ \tan^{-1}\left(\frac{x}{\tilde{\beta}_1}\right)\right]+(\omega\to-\omega)\right\}^{1}_{\tan[\gamma'/2]}$$

$$f_2(q,\omega) = \left[2q^2\left(\Delta_1^2+\Delta_2^2\right)-2(\Delta_s\Delta_d)^2\right]\left\{\frac{1}{2(q+\omega)q^2}\left[x-\frac{1}{\tilde{\beta}_1{}^2x}-\frac{\left(\tilde{\beta}_1{}^2+1\right)^2}{\tilde{\beta}_1{}^3}\tan^{-1}\left(\frac{x}{\tilde{\beta}_1}\right)\right]+(\omega\to-\omega)\right\}^{1}_{\tan[\gamma'/2]}$$

$$f_3(q,\omega) = \left\{\frac{-3(\Delta_s\Delta_d)^2}{8(q+\omega)q^2}\left[\frac{x^3}{3}-x\left(\tilde{\beta}_1{}^2+4\right)+\frac{4\tilde{\beta}_1{}^2+1}{\tilde{\beta}_1{}^4x}-\frac{1}{3\tilde{\beta}_1{}^2x^3}+\frac{\left(\tilde{\beta}_1{}^2+1\right)^4}{\tilde{\beta}_1{}^5}\tan^{-1}\left(\frac{x}{\tilde{\beta}_1}\right)\right]+(\omega\to-\omega)\right\}^{1}_{\tan[\gamma'/2]}.$$

While for $\omega > q$ regions, the result is expressed in terms of $g(q,\omega)$, whereas before it is expressed as the sum of three parts, $g(q,\omega) = g_1(q,\omega) + g_2(q,\omega) + g_3(q,\omega)$, which are given by

$$g_1(q,\omega) = \left(q^2+2\Delta_d^2\right)\left\{\frac{-2}{(q+\omega)}\left[\frac{1}{\tilde{\beta}_2}\ \ln\left(\frac{x+\tilde{\beta}_2}{|x-\tilde{\beta}_2|}\right)\right]+(\omega\to-\omega)\right\}^{1}_{\tan[\gamma'/2]}$$

$$g_2(q,\omega) = \left[2q^2\left(\Delta_1^2+\Delta_2^2\right)-2(\Delta_s\Delta_d)^2\right]\left\{\frac{-1}{2(q+\omega)q^2}\left[-x-\frac{1}{\tilde{\beta}_2{}^2x}+\frac{\left(\tilde{\beta}_2{}^2-1\right)^2}{\tilde{\beta}_2{}^3}\ln\left(\frac{x+\tilde{\beta}_2}{|x-\tilde{\beta}_2|}\right)\right]+(\omega\to-\omega)\right\}^{1}_{\tan[\gamma'/2]}$$

$$g_3(q,\omega) = \left\{\frac{3(\Delta_s\Delta_d)^2}{8(q+\omega)q^2}\left[-\frac{x^3}{3}-x\left(\tilde{\beta}_2{}^2-4\right)+\frac{4\tilde{\beta}_2{}^2-1}{\tilde{\beta}_2{}^4x}-\frac{1}{3\tilde{\beta}_2{}^2x^3}+\frac{\left(\tilde{\beta}_2{}^2-1\right)^4}{\tilde{\beta}_2{}^5}\ln\left(\frac{x+\tilde{\beta}_2}{|x-\tilde{\beta}_2|}\right)\right]+(\omega\to-\omega)\right\}^{1}_{\tan[\gamma'/2]},\tag{A4}$$

where $\gamma=\sqrt{q^2+\Delta_s^2}$, $\gamma'=\cos^{-1}[q/\gamma]$, $\tilde{\beta}_1{}^2=(q-\omega)/(q+\omega)$, $\tilde{\beta}_2{}^2=(\omega-q)/(q+\omega)$, and $(\omega\to-\omega)$ represent similar terms with sign of ω changed.

As a next step, $n_F[E_1(p)]$ terms from A_1 and A_3 are combined together and labeled as $\mathrm{Re}\Pi_{12-b}$:

$$\begin{aligned}\mathrm{Re}\,\Pi_{12-b} &= -\int\frac{d^2p}{(2\pi)^2}n_F[E_1(p)]\left\{\frac{E_1(p)+\omega}{[E_2(p+q)]^2-[E_1(p)+\omega]^2}+\left[\frac{\vec{p}_1\cdot(\vec{p}+\vec{q})_2}{E_1(p)}\right]\frac{1}{[E_2(p+q)]^2-[E_1(p)+\omega]^2}\right\}\\ &= -\frac{1}{4\pi}\left\{\int_{\Delta_1}^{\mu}\frac{dE_1}{\sqrt{\omega^2-q^2}}\left[\frac{\left((2E_1+\omega)^2-q^2-\Delta_d^2\right)\mathrm{sgn}[\alpha_b-E_1]}{\sqrt{(2E_1+\omega\gamma_b)^2-q^2\gamma_b^2+\frac{4q^2\Delta_1^2}{\omega^2-q^2}}}\right]+(\mu-\Delta_1)\right\}',\end{aligned}$$

where $\gamma_b=(\frac{\omega^2-q^2-\Delta_s\Delta_d}{\omega^2-q^2})$, $\alpha_b=(\frac{q^2+\Delta_s\Delta_d-\omega^2}{2\omega})$, and we have used $\int_0^{2\pi}d\phi/(a+b\cos\phi)=2\pi\ \mathrm{Sgn}[a]/\sqrt{a^2-b^2}$ to perform the angular integration. Due to the sgn function the result of the integration depends on the value of α_b with respect to the upper and lower limits; we obtain:

$$\text{(i)}\quad \alpha_b>\mu \quad\Rightarrow\quad \mathrm{Re}\,\Pi_{12-b}=-\frac{1}{4\pi}\Re\left[\frac{1}{\sqrt{\omega^2-q^2}}\{F_b(2\mu+\omega\gamma_b)-F_b(2\Delta_1+\omega\gamma_b)\}+(\mu-\Delta_1)\right]$$

$$\text{(ii)}\quad \mu>\alpha_b>\Delta_1 \quad\Rightarrow\quad \mathrm{Re}\,\Pi_{12-b}=-\frac{1}{4\pi}\Re\left[\frac{1}{\sqrt{\omega^2-q^2}}\{F_b(2\mu+\omega\gamma_b)+F_b(2\Delta_1+\omega\gamma_b)-2F_b(2\alpha_b+\omega\gamma_b)\}\right]$$

$$\text{(iii)}\quad \alpha_b<\Delta_1 \quad\Rightarrow\quad \mathrm{Re}\,\Pi_{12-b}=+\frac{1}{4\pi}\Re\left[\frac{1}{\sqrt{\omega^2-q^2}}\{F_b(2\mu+\omega\gamma_b)-F_b(2\Delta_1+\omega\gamma_b)\}+(\mu-\Delta_1)\right],\tag{A5}$$

where $\Re$ represents the real part of the corresponding function and

$$F_b(x)=\tfrac{1}{2}\left[\left(\xi_b^2-2\Delta_d^2-2q^2+2(\omega\gamma_b-\omega)^2\right)\log\left(\sqrt{x^2-\xi_b^2}+x\right)+(x-4(\omega\gamma_b-\omega))\sqrt{x^2-\xi_b^2}\right]$$

and $\xi_b=\sqrt{q^2\gamma_b^2-\frac{4q^2\Delta_1^2}{\omega^2-q^2}}$.

Finally the terms corresponding to $n_F[E_2(p+q)]$ from A_1 and A_2 are combined together into Re Π_{12-c}:

$$\begin{aligned}\text{Re}\,\Pi_{12-c} &= \int \frac{d^2p}{(2\pi)^2} n_F[E_2(p)]\left\{\frac{\omega - E_2(p)}{[E_1(p+q)]^2 - [E_2(p)-\omega]^2} - \left[\frac{(\vec{p}+\vec{q})_1 \cdot \vec{p}_2}{E_2(p)}\right]\frac{1}{[E_1(p+q)]^2 - [E_2(p)-\omega]^2}\right\} \\ &= -\frac{1}{4\pi}\left\{\int_{\Delta_2}^{\mu} \frac{dE_2}{\sqrt{\omega^2 - q^2}}\left[\frac{\left((2E_2-\omega)^2 - q^2 - \Delta_d^2\right)\text{Sgn}[E_2-\alpha_c]}{\sqrt{(2E_2-\omega\gamma_c)^2 - q^2\gamma_c^2 + \frac{4q^2\Delta_2^2}{\omega^2-q^2}}}\right] + (\mu - \Delta_2)\right\},\end{aligned}$$

where $\gamma_c = (\frac{\omega^2-q^2+\Delta_s\Delta_d}{\omega^2-q^2})$ and $\alpha_c = (\frac{\omega^2-q^2+\Delta_s\Delta_d}{2\omega})$. As before, due to the sgn function, the integral yields three different results depending on the value of α_c. They are

$$\begin{aligned}&\text{(i)}\quad \alpha_c > \mu \quad \Rightarrow \quad \text{Re}\,\Pi_{12-c} = +\frac{1}{4\pi}\Re\left[\frac{1}{\sqrt{\omega^2-q^2}}\{F_c(2\mu-\omega\gamma_c) - F_c(2\Delta_2-\omega\gamma_c)\} + (\mu-\Delta_2)\right] \\ &\text{(ii)}\quad \mu > \alpha_c > \Delta_2 \quad \Rightarrow \quad \text{Re}\,\Pi_{12-c} = -\frac{1}{4\pi}\Re\left[\frac{1}{\sqrt{\omega^2-q^2}}\{F_c(2\mu-\omega\gamma_c) + F_c(2\Delta_2-\omega\gamma_c) - 2F_c(2\alpha_c-\omega\gamma_c)\}\right] \\ &\text{(iii)}\quad \alpha_c < \Delta_2 \quad \Rightarrow \quad \text{Re}\,\Pi_{12-c} = -\frac{1}{4\pi}\Re\left[\frac{1}{\sqrt{\omega^2-q^2}}\{F_c(2\mu-\omega\gamma_c) - F_c(2\Delta_2-\omega\gamma_c)\} + (\mu-\Delta_2)\right],\end{aligned} \tag{A6}$$

where

$$F_c(x) = \tfrac{1}{2}\left[\left(\xi_c^2 - 2\Delta_d^2 - 2q^2 + 2(\omega\gamma_c-\omega)^2\right)\log\left(\sqrt{x^2-\xi_c^2}+x\right) + (x + 4(\omega\gamma_c-\omega))\sqrt{x^2-\xi_c^2}\right],$$

and $\xi_c = \sqrt{q^2\gamma_c^2 - \frac{4q^2\Delta_2^2}{\omega^2-q^2}}$.

Similar to the earlier derivation we will next integrate the terms of Eq. (5) by considering the contributions from $\Delta_2 \to \Delta_1$ transition by considering $\beta = -1$ and $\beta' = +1$ (in the case of K valley), for all possible values of α and α'. As before, we divide the real part of polarization operator $\Pi(q, w)$ as follows,

$$\begin{aligned}B_1 &= -\frac{1}{2}\int \frac{d^2p}{(2\pi)^2}\left(1 + \frac{\vec{p}_2\cdot(\vec{p}+\vec{q})_1}{E_2(p)\cdot E_1(p+q)}\right)\left[\frac{n_F[E_2(p)]}{-E_2(p)+E_1(p+q)-\omega} - \frac{n_F[E_1(p+q)]}{-E_2(p)+E_1(p+q)-\omega}\right] \\ B_2 &= -\frac{1}{2}\int \frac{d^2p}{(2\pi)^2}\left(1 - \frac{\vec{p}_2\cdot(\vec{p}+\vec{q})_1}{E_2(p)\cdot E_1(p+q)}\right)\left[\frac{1}{+E_2(p)+E_1(p+q)-\omega} - \frac{n_F[E_1(p+q)]}{+E_2(p)+E_1(p+q)-\omega}\right] \\ B_3 &= -\frac{1}{2}\int \frac{d^2p}{(2\pi)^2}\left(1 - \frac{\vec{p}_2\cdot(\vec{p}+\vec{q})_1}{E_2(p)\cdot E_1(p+q)}\right)\left[\frac{n_F[E_2(p)]}{-E_2(p)-E_1(p+q)-\omega} - \frac{1}{-E_2(p)-E_1(p+q)-\omega}\right],\end{aligned}$$

The first term of B_2 and the second term of B_3 yield terms that are independent of μ; we combine them together and represent it as Re Π_{21-a}. Performing the following change of variables $p+q \to p$ and $p \to -p$ it is easy to show that $\text{Re}\Pi_{21-a}(q,\omega) = \text{Re}\Pi_{12-a}(q,\omega)$. The combined contribution represented as $\text{Re}\Pi_a$ is thus given by $\text{Re}\Pi_a = \text{Re}\Pi_{21-a}(q,\omega) + \text{Re}\Pi_{12-a}(q,\omega)$.

Similar to the evaluation of Re Π_{12-b}, we combine terms corresponding to $n_F[E_1(p+q)]$ from B_1 and B_2 and denote the contributions as Re Π_{21-b}. A change of variables as above yields

$$\text{Re}\,\Pi_{21-b}(q,\omega) = -\int \frac{d^2p}{(2\pi)^2} n_F[E_1(p)]\left\{\frac{E_1(p)-\omega}{[E_2(p+q)]^2 - [E_1(p)-\omega]^2} + \left[\frac{\vec{p}_1\cdot(\vec{p}+\vec{q})_2}{E_1(p)}\right]\frac{1}{[E_2(p+q)]^2 - [E_1(p)-\omega]^2}\right\},$$

thus Re $\Pi_{21-b}(q,\omega) = \text{Re}\,\Pi_{12-b}(q,-\omega)$. The total contribution is Re $\Pi_b(q,\omega) = \text{Re}\,\Pi_{12-b}(q,\omega) + \text{Re}\,\Pi_{21-b}(q,\omega)$. Following essentially the same arguments we obtain Re $\Pi_{21-c}(q,\omega) = \text{Re}\,\Pi_{12-c}(q,-\omega)$, thus Re $\Pi_c(q,\omega) = \text{Re}\,\Pi_{12-c}(q,\omega) +$ Re $\Pi_{21-c}(q,\omega)$. Therefore, the full result for $\text{Re}\Pi_{xx/yy}$ is

$$\text{Re}\Pi_{xx/yy}(q,\omega) = \text{Re}\Pi_a(q,\omega) + \text{Re}\Pi_b(q,\omega) + \text{Re}\Pi_c(q,\omega). \tag{A7}$$

2. Re $\Pi_{xx,yy}(q, \omega = 0)$

We will use the expression of $\text{Re}\Pi_{xx,yy}(q,\omega)$ as given in Appendix 1 to obtain the $\omega = 0$ limit. As before, $\text{Re}\Pi_{xx,yy}$ can be expressed as the sum of three components, $\text{Re}\Pi_{xx,yy}(q) = \text{Re}\Pi_a(q) + \text{Re}\Pi_b(q) + \text{Re}\Pi_c(q)$. The results of the calculations for

the individual terms are as follows. The integral without the chemical potential term is given by

$$\mathrm{Re}\,\Pi_a(q) = -\frac{1}{8\pi}(f_1 + f_2 + f_3), \tag{A8}$$

where the lower limit on all three integrals are $l = \tan[\frac{1}{2}\cos^{-1}(\frac{q}{\sqrt{q^2+\Delta_s^2}})]$,

$$f_1(q,0) = \frac{4}{q}\left[q^2 + 2\Delta_d^2\right][\tan^{-1}(x)]_l^1, \tag{A9}$$

$$f_2(q,0) = \frac{1}{q^3}\left[2q^2\left(\Delta_1^2 + \Delta_2^2\right) - 2(\Delta_s\Delta_d)^2\right]\left[x - \frac{1}{x} - 4\tan^{-1}(x)\right]_l^1,$$

$$f_3(q,0) = -\frac{3(\Delta_s\Delta_d)^2}{4q^3}\left[\frac{x^3}{3} - 5x + \frac{5}{x} - \frac{1}{3x^3} + 2^4\tan^{-1}(x)\right]_l^1. \tag{A10}$$

Combining them together we obtain, $\mathrm{Re}\,\Pi_a(q) = -\frac{\Delta_d^2+q^2}{4\pi q^3}\{[q^2 - \Delta_s^2]\tan^{-1}(\frac{q}{\Delta_s}) + q\Delta_s\}$.

$\mathrm{Re}\Pi_b(q)$ includes contributions from all integrals that have $n_F[E_1(p)]$ and $n_F[E_1(p+q)]$ terms:

$$\mathrm{Re}\,\Pi_b(q) = -\frac{1}{2\pi}\left\{\mu - \Delta_1 + \int_{\Delta_1}^{\mu}\frac{dx}{2q}\frac{\left[4x^2 - q^2 - \Delta_d^2\right]\mathrm{sgn}(q^2 + \Delta_s\Delta_d)}{\sqrt{\xi^2 - x^2}}\right\}, \tag{A11}$$

where $\xi = \sqrt{\frac{\left(q^2+\Delta_s\Delta_d\right)^2 + 4q^2\Delta_1^2}{4q^2}}$. The result of the integration is given in Eq. (33) of the main text. The last term, $\mathrm{Re}\Pi_c(q)$, includes contributions from all integrals containing $n_F[E_2(p)]$ and $n_F[E_2(p+q)]$ terms and is given by

$$\mathrm{Re}\,\Pi_c(q) = -\frac{1}{2\pi}\left\{\mu - \Delta_2 + \int_{\Delta_2}^{\mu}\frac{dx}{2q}\frac{\left[4x^2 - q^2 - \Delta_d^2\right]\mathrm{sgn}(q^2 - \Delta_s\Delta_d)}{\sqrt{\xi^2 - x^2}}\right\}. \tag{A12}$$

The final result for $\mathrm{Re}\,\Pi_c(q)$ is obtained from $\mathrm{Re}\,\Pi_b(q)$ by exchanging Δ_1 with Δ_2 and vice versa. Adding together the three terms we find that the static part of the polarization function has a constant value for $q < k_{F_1} + k_{F_2}$, while the change in polarization function from the constant value for $q > k_{F_1} + k_{F_2}$ is given by

$$\delta[\mathrm{Re}\Pi_{xx,yy}(q)] = \frac{1}{2\pi}\left[\frac{\mu\sqrt{\left(q^2 - q_d^2\right)\left(q^2 - q_s^2\right)}}{q^2} - \frac{\left(q^2 + \Delta_d^2\right)\left(q^2 - \Delta_s^2\right)}{2q^3}\tan^{-1}\left(\frac{\sqrt{\left(q^2 - q_d^2\right)\left(q^2 - q_s^2\right)}}{2\mu q}\right)\right], \tag{A13}$$

where $q_s = k_{F_1} + k_{F_2}$ and $q_d = k_{F_1} - k_{F_2}$.

3. Derivation of Re $\Pi_{xx,yy}(\mathbf{q} = 0, \omega)$

The Im $\Pi_a(\omega)$ term with contributions from both $\Delta_1 \to \Delta_2$ and $\Delta_2 \to \Delta_1$ transitions is given by

$$\mathrm{Im}\,\Pi_a(\omega) = -\frac{1}{8}\Theta\left(\omega^2 - \Delta_s^2\right)\mathrm{Y}(\omega); \quad \mathrm{Y}(\omega) = \frac{2\Delta_d^2}{\omega}\left[1 - \frac{\Delta_s^2}{\omega^2}\right]. \tag{A14}$$

Utilizing the Kramers-Kronig relation we obtain for $\mathrm{Re}\,\Pi_a(\omega)$

$$\mathrm{Re}\,\Pi_a(\omega) = \frac{1}{\pi}\mathrm{P}\int_{-\infty}^{\infty}d\omega'\frac{\mathrm{Im}\,\Pi_a(\omega')}{(\omega' - \omega)}\,\mathrm{sgn}(\omega') = -\frac{\Delta_d^2}{4\pi\omega}\left\{\log\left[\frac{\Delta_s + \omega}{|\Delta_s - \omega|}\right]\left(1 - \frac{\Delta_s^2}{\omega^2}\right) + \frac{2\Delta_s}{\omega}\right\}.$$

A direct integration by considering contributions from the integrals containing $n_F(E_1)$ term yields

$$\begin{aligned}
\mathrm{Re}\,\Pi_b &= -\int\frac{d^2p}{(2\pi)^2}n_F[E_1(p)]\left\{\frac{E_1(p) + \omega}{[E_2(p)]^2 - [E_1(p) + \omega]^2} + \left[\frac{\vec{p}_1\cdot\vec{p}_2}{E_1(p)}\right]\frac{1}{[E_2(p)]^2 - [E_1(p) + \omega]^2}\right\} + [\omega \to -\omega] \\
&= -\frac{1}{4\pi}\left\{\int_{\Delta_1}^{\mu}dE_1\left[\frac{(2E_1 + \omega)^2 - \Delta_d^2}{\Delta_s\Delta_d - \omega^2 - 2E_1\omega}\right] + [\omega \to -\omega]\right\} - \frac{(\mu - \Delta_1)}{2\pi} \\
&= -\frac{1}{4\pi}\left\{\frac{\Delta_d^2(\Delta_s^2 - \omega^2)}{2\omega^3}\left(\log\left[\frac{(-\Delta_d\Delta_s - 2\mu\omega + \omega^2)(-\Delta_d\Delta_s + 2\omega\Delta_1 + \omega^2)}{(-\Delta_d\Delta_s + 2\mu\omega + \omega^2)(-\Delta_d\Delta_s - 2\omega\Delta_1 + \omega^2)}\right]\right) - \frac{2\Delta_d\Delta_s(\mu - \Delta_1)}{\omega^2}\right\}.
\end{aligned} \tag{A15}$$

Similarly, $n_F(E_2)$ term yields a contribution to Re Π_c given by

$$\begin{aligned}\text{Re}\,\Pi_c &= -\int \frac{d^2p}{(2\pi)^2} n_F[E_2(p)]\left\{\frac{E_2(p)-\omega}{[E_1(p)]^2-[E_2(p)-\omega]^2}+\left[\frac{\vec{p}_1\cdot\vec{p}_2}{E_2(p)}\right]\frac{1}{[E_1(p)]^2-[E_2(p)-\omega]^2}\right\}+[\omega\to-\omega]\\ &= -\frac{1}{4\pi}\left\{\int_{\Delta_2}^{\mu} dE_2\left[\frac{(2E_2-\omega)^2-\Delta_d^2}{-\Delta_s\Delta_d-\omega^2+2E_2\omega}\right]+[\omega\to-\omega]\right\}-\frac{(\mu-\Delta_2)}{2\pi}\\ &= -\frac{1}{4\pi}\left\{\frac{\Delta_d^2(\Delta_s^2-\omega^2)}{2\omega^3}\left(\log\left[\frac{(\Delta_d\Delta_s-2\mu\omega+\omega^2)(\Delta_d\Delta_s+2\omega\Delta_2+\omega^2)}{(\Delta_d\Delta_s+2\mu\omega+\omega^2)(\Delta_d\Delta_s-2\omega\Delta_2+\omega^2)}\right]\right)+\frac{2\Delta_d\Delta_s(\mu-\Delta_2)}{\omega^2}\right\}. \qquad \text{(A16)}\end{aligned}$$

[1] G. Dresselhaus, Phys. Rev. **100**, 580 (1955).
[2] S. Datta and B. Das, Appl. Phys. Lett. **56**, 665 (1990).
[3] I. Žutić, J. Fabian, and S. Das Sarma, Rev. Mod. Phys. **76**, 323 (2004).
[4] C.-C. Liu, W. Feng, and Y. Yao, Phys. Rev. Lett. **107**, 076802 (2011).
[5] S. Raghu, S. B. Chung, X.-L. Qi, and S.-C. Zhang, Phys. Rev. Lett. **104**, 116401 (2010).
[6] P. Di Pietro, M. Ortolani, O. Limaj, A. Di Gaspare, V. Giliberti, F. Giorgianni, M. Brahlek, N. Bansal, N. Koirala, S. Oh, P. Calvani, and S. Lupi, Nat. Nanotechnol. **8**, 556 (2013).
[7] J. Hofmann and S. Das Sarma, Phys. Rev. B **91**, 241108(R) (2015).
[8] I. Panfilov, A. A. Burkov, and D. A. Pesin, Phys. Rev. B **89**, 245103 (2014).
[9] J. Zhou, H.-R. Chang, and D. Xiao, Phys. Rev. B **91**, 035114 (2015).
[10] Q. H. Wang, K. Kalantar-Zadeh, A. Kis, J. N. Coleman, and M. S. Strano, Nat. Nanotechnol. **7**, 699 (2012).
[11] M. Ezawa, J. Phys. Soc. Jpn. **84**, 121003 (2015).
[12] P. Vogt, P. De Padova, C. Quaresima, J. Avila, E. Frantzeskakis, M. C. Asensio, A. Resta, B. Ealet, and G. Le Lay, Phys. Rev. Lett. **108**, 155501 (2012).
[13] B. Lalmi, H. Oughaddou, H. Enriquez, A. Kara, S. Vizzini, B. Ealet, and B. Aufray, Appl. Phys. Lett. **97**, 223109 (2010).
[14] C.-C. Liu, H. Jiang, and Y. Yao, Phys. Rev. B **84**, 195430 (2011).
[15] C. L. Kane and E. J. Mele, Phys. Rev. Lett. **95**, 226801 (2005).
[16] B. A. Bernevig, T. L. Hughes, and S.-C. Zhang, Science **314**, 1757 (2006).
[17] N. D. Drummond, V. Zólyomi, and V. I. Fal'ko, Phys. Rev. B **85**, 075423 (2012).
[18] M. Ezawa, New J. Phys. **14**, 033003 (2012).
[19] M. Ezawa, Phys. Rev. Lett. **109**, 055502 (2012).
[20] C. J. Tabert and E. J. Nicol, Phys. Rev. B **89**, 195410 (2014).
[21] C. J. Tabert, J. P. Carbotte, and E. J. Nicol, Phys. Rev. B **91**, 035423 (2015).
[22] M. Ezawa, Phys. Rev. B **87**, 155415 (2013).
[23] C. J. Tabert and E. J. Nicol, Phys. Rev. B **87**, 235426 (2013).
[24] F. Stern, Phys. Rev. Lett. **18**, 546 (1967).
[25] T. Ando, A. B. Fowler, and F. Stern, Rev. Mod. Phys. **54**, 437 (1982).
[26] G.-H. Chen and M. E. Raikh, Phys. Rev. B **59**, 5090 (1999).
[27] M. Pletyukhov and V. Gritsev, Phys. Rev. B **74**, 045307 (2006).
[28] K. W.-K. Shung, Phys. Rev. B **34**, 979 (1986).
[29] E. V. Gorbar, V. P. Gusynin, V. A. Miransky, and I. A. Shovkovy, Phys. Rev. B **66**, 045108 (2002).
[30] R. Roldán and L. Brey, Phys. Rev. B **88**, 115420 (2013).
[31] P. K. Pyatkovskiy, J. Phys.: Condens. Matter **21**, 025506 (2009).
[32] A. Scholz, T. Stauber, and J. Schliemann, Phys. Rev. B **86**, 195424 (2012).
[33] Y. Barlas, T. Pereg-Barnea, M. Polini, R. Asgari, and A. H. MacDonald, Phys. Rev. Lett. **98**, 236601 (2007).
[34] E. H. Hwang and S. Das Sarma, Phys. Rev. B **75**, 205418 (2007).
[35] V. N. Kotov, B. Uchoa, V. M. Pereira, F. Guinea, and A. H. Castro Neto, Rev. Mod. Phys. **84**, 1067 (2012).
[36] A. Shekhter, M. Khodas, and A. M. Finkel'stein, Phys. Rev. B **71**, 165329 (2005).
[37] S. Chesi and D. Loss, Phys. Rev. B **82**, 165303 (2010).
[38] A. Ashrafi and D. L. Maslov, Phys. Rev. Lett. **109**, 227201 (2012).
[39] S. Maiti, V. Zyuzin, and D. L. Maslov, Phys. Rev. B **91**, 035106 (2015).
[40] H. Imamura, P. Bruno, and Y. Utsumi, Phys. Rev. B **69**, 121303(R) (2004).
[41] J. Klinovaja and D. Loss, Phys. Rev. B **87**, 045422 (2013).
[42] H.-J. Duan, C. Wang, S.-H. Zheng, R.-Q. Wang, D.-R. Pan, and M. Yang, Sci. Rep. **8**, 6185 (2018).
[43] T. Kushida, J. C. Murphy, and M. Hanabusa, Phys. Rev. B **13**, 5136 (1976).
[44] G. Giuliani and G. Vignale, *Quantum Theory of the Electron Liquid* (Cambridge University Press, New York, 2005).
[45] C. P. Slichter, *Principles of Nuclear Resonance* (Springer-Verlag, Heidelberg, 1990).
[46] V. M. Pudalov, M. E. Gershenson, H. Kojima, N. Butch, E. M. Dizhur, G. Brunthaler, A. Prinz, and G. Bauer, Phys. Rev. Lett. **88**, 196404 (2002).
[47] K. Vakili, Y. P. Shkolnikov, E. Tutuc, E. P. De Poortere, and M. Shayegan, Phys. Rev. Lett. **92**, 226401 (2004).
[48] O. Gunawan, Y. P. Shkolnikov, K. Vakili, T. Gokmen, E. P. De Poortere, and M. Shayegan, Phys. Rev. Lett. **97**, 186404 (2006).
[49] S. W. Lovesey, *Theory of Neutron Scattering from Condensed Matter* (Clarendon Press, Oxford, 1986).
[50] H.-H. Kung, S. Maiti, X. Wang, S.-W. Cheong, D. L. Maslov, and G. Blumberg, Phys. Rev. Lett. **119**, 136802 (2017).
[51] H.-R. Chang, J. Zhou, H. Zhang, and Y. Yao, Phys. Rev. B **89**, 201411(R) (2014).

[52] B. Van Duppen, P. Vasilopoulos, and F. M. Peeters, Phys. Rev. B **90**, 035142 (2014).
[53] M. Ezawa, Eur. Phys. J. B **85**, 363 (2012).
[54] A. Thakur, R. Sachdeva, and A. Agarwal, J. Phys.: Condens. Matter **29**, 105701 (2017).
[55] N. F. Berk and J. R. Schrieffer, Phys. Rev. Lett. **17**, 433 (1966).
[56] S. Doniach and S. Engelsberg, Phys. Rev. Lett. **17**, 750 (1966).
[57] H.-R. Chang, J. Zhou, S.-X. Wang, W.-Y. Shan, and D. Xiao, Phys. Rev. B **92**, 241103(R) (2015).
[58] E. Kogan, Phys. Rev. B **84**, 115119 (2011).